Università degli Studi di Udine

Dottorato di Ricerca in Matematica e Fisica - XXVII Ciclo

Anno Accademico 2015/2016

On the connection between radio and gamma-ray emission in Active Galactic Nuclei

Ph.D. Thesis

Dottorando: Pietro Leonardo Cerchiara

Relatore: Prof. Alessandro De Angelis

Università di Udine

May 18, 2016

Contents

Glossary

2LAC The Second LAT AGN Catalog . 42

AT20G Australia Telescope 20 GHz . 50

ATCA Australia Telescope Compact Array . 51

BH Black Hole. 24

Chandra The Chandra X-ray Observatory (CXO) have the name in honor of Nobel Prizewinning Indian-American astrophysicist Subrahmanyan Chandrasekhar. 28

FSRQ Flat Spectrum Radio Quasars. 27

HESS High Energy Stereoscopic System. 16

LAT Large Area Telescope. 15

LOFAR Low Frequency Array . 79

MAGIC Major Atmospheric Gamma-ray Imaging Cherenkov Telescope. 16

MILAGRO The spanish word for miracle. 16

PKS Parkes Radio Sources . 6, 56

SKA Square Kilometre Array . 79

SSRQ Steep-Spectrum Radio Quasars. 27

VERITAS Very Energetic Radiation Imaging Telescope Array System. 16

Prologo

"Ogni atomo ponderabile e' differenziato da un fluido tenue, che riempie tutto lo spazio meramente con un moto rotatorio, proprio come fa un vortice di acqua in un lago calmo. Una volta che questo fluido viene messo in movimento, esso diventa grossolana materia. Non appena il suo movimento viene arrestato la sostanza primaria ritorna al suo stato normale... Puo' allora accadere che, se riesce in qualche modo a imbrigliare questo fluido, l'uomo possa innescare o fermare questi suoi vortici in movimento in modo da creare alternativamente la formazione e sparizione della materia. Dunque al suo comando, quasi senza sforzo da parte sua, vecchi mondi svanirebbero e nuovi mondi entrerebbero nell'esistenza. L'uomo potrebbe cos alterare le dimensioni di questo pianeta, controllare le sue stagioni, aggiustare la sua distanza dal Sole, guidarlo nel suo viaggio eterno lungo l'orbita di sua scelta, attraverso le profondita' dell'universo. Egli potrebbe far collidere i pianeti e creare i suoi soli e le sue stelle, il suo calore e la sua luce, egli potrebbe dare origine alla vita in tutte le sue infinite forme. Tutto questo gli permetterebbe di compiere il suo destino ultimo." (Nikola Tesla)

Ringrazio il Relatore di questa tesi, Prof. Alessandro De Angelis, il Prof. Daniele Dallacasa del Dipartimento di Fisica e Astronomia dell'Universitá di Bologna, per preziosi suggerimenti ed il Dott. Marco Pavan del Dipartimento d'Informatica dell'Universitá di Udine, per il supporto informatico.

Abstract

The extragalactic gamma-ray sky is largely dominated by radio-loud active galactic nuclei (AGN). In particular, the population of blazars represents almost 97 % of the gamma-ray emitting AGN. Blazars, the most extreme class of Active Galactic Nuclei (AGNs), are observed at almost the full electromagnetic spectrum from radio to gamma-ray band.

A connection between the radio and gamma-ray emission in blazars has long been suspected, and has received renewed attention during the era of the Fermi Large Area Telescope (LAT) . It is straightforward to demonstrate a statistically significant correlation between observed gamma-ray and radio luminosities or flux densities, as was done during the era of the EGRET instrument. Recent studies using LAT data and concurrent or nearly concurrent radio data provide stronger evidence for an intrinsic correlation.

In this thesis we have searched for a correlation between radio and gamma-rays emissions in a sample of 174 blazars extracted from the 2FGL catalogue, of which 132 quasars and 7 BLLac, with the predominance of sources in the Southern Emisphere, extracted from the PKS Catalog Cat90, associated to radio sources with F5GHz < 6 Jy.

Using the probably correlation between the brightness and the radio VHE and considering the expected sensitivity of the future Cherenkov Telescope Array, we have also estimated that with this system of telescopes it will be possible to reveal at least 82 radio galaxies, extracted from various catalogs radio to the frequency of 5 GHz. Definitely a considerable increase in number respect to those actually observed with HESS and MAGIC telescopes. This number, which is therefore of the order of hundreds, is an estimate because both the sites and the configurations of the telescopes of the CTA are not yet fully defined. From the analysis of the estimate of the distribution of radio galaxies as a function of the redshift we have also observed that the majority of them is located at distances z between 0.01 and 0.05, so relatively close.

1 Introduction

1.1 Radio astronomy

Radio astronomy is the branch of astronomy that investigates celestial object in the range of radio frequencies. It was born in the 1930s, when the detection of radio waves from an astronomical object led to discovery of the source Sagittarius A in the densest part of the Milky Way. The frequency range and the polarization led Jansky to rule out thermal emission from galactic gas and dust. This emission arise from free electrons embedded in a strong magnetic field, originated from the complex of objects found in the neighbourhood of the galactic center. From that time on, observations have identified some different sources responsible for radio emission. This emission is totally non-thermal and often come out from jets and jet-like structures, so that it is intrinsically different from thermal emission revealed. The physics governing the radio emission scenario is directly linked to the accretion phenomena, especially for what concerns the jet formation, as a result of unstable modes taking place in the increased plasma.

1.2 Emission mechanism

1.2.1 Synchrotron radiation

The main source of detected non-thermal radio waves is synchrotron radiation, generated by astronomical objects because of relativistic electrons spiraling through magnetic fields. It features broad-band power-law emission spectra and a strong degree of polarization. For non-relativistic motion (cyclotron radiation), the radiation spectrum shows a main spike at the fundamental frequency corresponding to the orbital motion, called the gyration frequency

$$f_c = \frac{eB}{m_e c} \tag{1}$$

where e and m_e are electronic charge and electronic mass, respectively. For this emission to be strong enough to have an astronomical significance, the electrons must be traveling at nearly the speed of light, i.e. with Lorentz factor $\gamma \gg 1$; in this case, the radiation is compressed into a small range of angles γ^{-1} around the instantaneous velocity vector of the particle. This is called "relativistic beaming". Figure 1 shows a picture of the process.

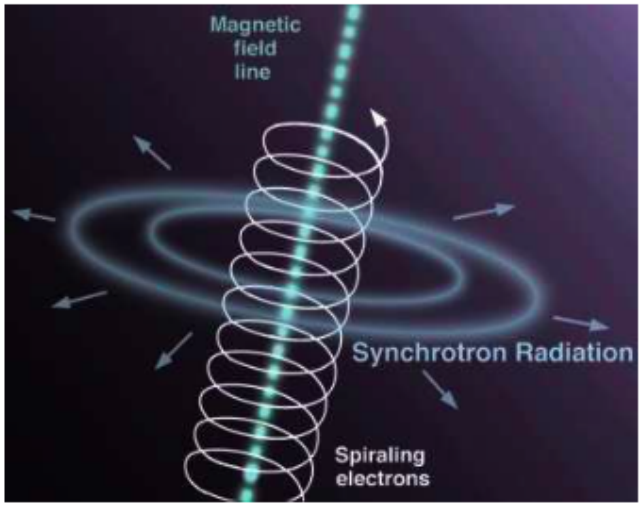

Figure 1: Overview of the synchrotron physical process

1.3 Relativistic Beaming

If the source of radio emission is moving near the speed of light along a direction which lies close to the line of sight, then the source nearly catches up with its own radiation. This can give the illusion of apparent transverse motion at a speed greater than the speed of light. If the true velocity is v and is at an angle, theta, with respect to the line of sight, then the apparent velocity, $v(a)$ is given by

$$v(a) = \frac{v \sin\theta}{1 - \beta \cos\theta}, \tag{2}$$

where

$$\beta = \frac{v}{c}. \tag{3}$$

Defining the relativistic Doppler factor as $\delta \equiv \left[\gamma_j(1 - \beta_j \cos\theta_j)\right]^{-1}$ and the jet speed normalized to the speed of light,

$$\gamma_j = \frac{1}{\sqrt{1 - \beta_j^2}}, \tag{4}$$

the observed and intrinsic luminosities at a given frequency f are related by

$$L_f(obs) = \delta^p L_f(em) \tag{5}$$

with p from 2 to 3, and the variability timescales are related by

$$\delta_{tobs} = \delta^{-1} \delta_{tem}. \tag{6}$$

For $\theta = \theta_0$ and $\delta = 2\gamma_j$ the observed luminosity can be amplified by factors from 400 to 10^4 (for typically $\gamma_j = 10$ and p= 2-3); whereas $\theta_j = \frac{1}{\gamma_j}$ implies $\delta = \gamma_j$, with a luminosity amplification from 10^2 to 10^3.

1.3.1 Inverse Compton

The mechanism wherein a photon gains energy as a result of a reaction with a moving electron is called Inverse Compton mechanism. Although the total radiation field is fairly isotropic in the rest frame of the source, it is extremely anisotropic when looking at the individual ultra-relativistic electrons producing the synchrotron emission; nearly all ambient photons are emitted within an angle γ^{-1} because of relativistic aberration. Thomson scattering of this highly anisotropic emission reduces the electron kinetic energy and converts it into Inverse-Compton (IC) radiation by up-scattering radio emission to become optical or X-ray emission. E.g., isotropic radio emission at f=1 GHz, IC-scattered by electrons having $\gamma = 10^4$, will be up-scattered to the average frequency

$$f_a = 4\gamma^2 f/3 = 1.3 \times 10^{17} \text{Hz} \tag{7}$$

corresponding to X-ray radiation.
Figure 2 shows a picture of the Inverse Compton process.

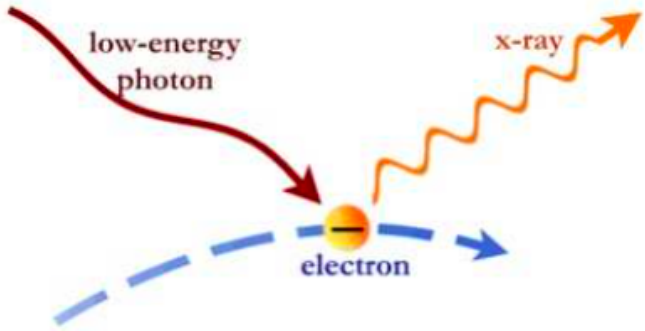

Figure 2: Overview of the Inverse Compton process

1.4 Radio detectors

The main research instruments in radio astronomy are large antennas referred to as radio telescopes, generally used singularly or in an array. When used in an array supplementary techniques like radio interferometry and aperture synthesis are adopted.
Observations from Earth's surface are limited to wavelengths that can pass through the ionosphere, which reflects waves with frequencies less than its characteristic plasma frequency, while water vapor absorption interferes at higher frequencies. The "radio window" spans wavelengths from centimeters to tens of meters, and is three orders of magnitude wider than its optical and infrared counterparts. Because to this wide range, radio telescopes vary in design, size and configuration. Instruments operating at less than 30 cm range in size from 3 to 90 m and instruments working from 30 cm to 3 m have usually size over 100 meters in diameter. Radio interferometers consist of array of radio telescopes, widely separated and usually connected using some type of transmission line or by independent recording of the signals at the various antennas, and later correlating the recordings in a process known as Very Long Baseline Interferometry (VLBI). This increase the total signal collected and the resolution through the aperture synthesis in the superposition principle. This eventually creates a combined telescope equivalent in resolution (tough not in sensitivity) to a single telescope whose diameter is equal to the spacing of the antennas furthest apart in the array (it does not collect as many radio waves as a large instrument of that size).

Figure 3 shows a photo of a parabolic VLBI radio antenna.

Figure 3: The VLBI antenna at the Nuffield Radio Astronomy Laboratories in Jodrell Bank (England)

1.5 Gamma-ray astrophysics

About one century ago, two works by Victor Hess (Nobel Prize in 1936), and by Domenico Pacini (his fundamental work was performed at the same time independently and with different techniques) proved that a flow of high-energy particles reaching the Earth was of extraterrestrial origin. This flow of particles was called "cosmic rays". Cosmic rays are messengers of the non thermal universe, because their energies exceed the temperature ordinarily encountered in astronomical objects. Excluding neutrinos, cosmic rays mainly consist of charged particles: protons (about 90%), helium nuclei ($< 10\%$) , electrons ($< 1\%$), and ionized heavier elements ($< 1\%$). Cosmic rays consist also of photons with energy > 1 MeV (only $0.1 - 1\%$); for historical reasons these are called "gamma-rays". The energy of cosmic rays range from tens of MeV up to 10^{20} eV and higher and the dependence of the flux on the energy E of the particles can be approximated by a power law

$$\frac{dN}{dE} \propto E^{-\alpha} \tag{8}$$

where the spectral index α has typical values between 2.5 and 3. Figure 4 shows the energy spectrum for cosmic rays.

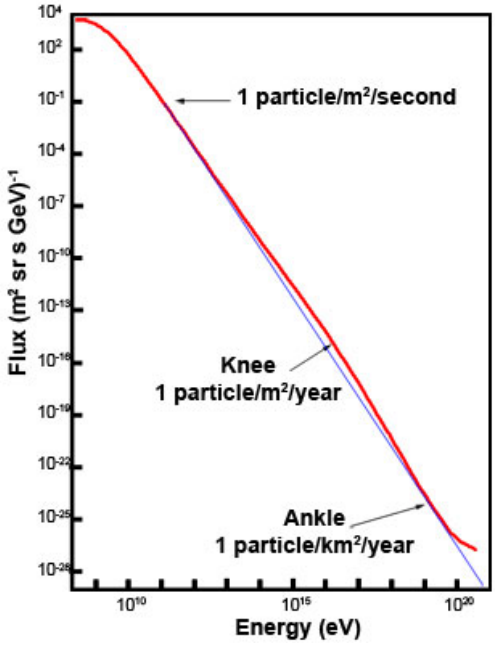

Figure 4: Overview of the comic rays energies

Gamma-rays are a very interesting part of the spectrum of photon emission from astronomical sources. A new window has been opened in the observation of gamma-rays above 20 MeV during the recent years, thanks to the availability of new photon detectors coming from technologies of experimental particle physics. Such photons are called High-Energy (HE) gamma-rays. This arbitrary definition reflects profound astrophysical and experimental arguments:

- the emission is non-thermal and dominated by the conversion of gravitational energy into electromagnetic energy;
- is impossible to concentrate the photons, so the telescopes are radically different from the ones dedicated to observation of larger wavelengths;
- charged cosmic particles produce large quantity of background events.

An other arbitrary classification of the gamma-rays is: High-Energy (HE), Very-High-Energy (VHE), Ultra-High-Energy (UHE), and Extremely-High-Energy (EHE) gamma-rays. The energy ranges associated are, respectively: 20 MeV-30 GeV; 30 GeV-30 TeV; 30 TeV-30 PeV; 30 PeV-no limit.

1.6 Production processes of gamma-rays

The gravitational energy released by collapses toward a central massive object is the source of high-energy photons coming from astrophysical objects. The dynamic of this collapse can manifest itself in an accretion disk, with the presence of jets of plasma outflowing the accretion disk, if it is present a non zero angular momentum. Charged particles, generally electrons, mostly generate the photon radiation which is at the origin of the production of gamma-rays. Such radiation can be due to:

- Synchrotron radiation.
- Bremsstrahlung.

In an external field an electron radiates because of the bremsstrahlung which present a characteristic spectrum proportional to $1/E$, where E is the energy of the emitted photon.

1.6.1 Photons from gravitational collapses

The production of high-energy photons from gravitational collapses is interpreted as the so-called Self-Synchrotron Compton (SSC) mechanism. Synchrotron emission from ultra-relativistic electrons accelerated in a magnetic field generate photons with an energy spectrum peaked in the infrared/X-ray range. Such photons interact via Compton scattering with their own parent electron population; the up-scattering of low-energy photons by collisions with high-energy electrons is the Inverse Compton (IC) scattering. This mechanism increases the photon energy (for this reason it is called "inverse"), and is very important in regions of soft-photon energy density and energetic-electron number density.

1.7 Propagation of gamma-rays

A source of opacity of the Universe to gamma-rays is the electron-positron (e^+e^-) pair production in the interaction of beam photons of extragalactic background photons, whenever the corresponding photon mean free path is smaller than the source distance. The probability for a photon of observed energy E to survive absorption along its path from its source at redshift z to the observer is usually expressed in the form

$$e^{-\tau}(E, z) \tag{9}$$

and it plays the role of an attenuation factor for the radiation flux. The coefficient τ is called "optical depth".

1.8 Detection techniques for HE gamma-ray

When compared to the corresponding charged particles of similar energy, the detection of high-energy photons is complicated by the absorption by the atmosphere and by the faintness of the signal. Only satellite-based detectors can detect primary X/gamma-rays. VHE and UHE gamma-rays can be detected only from the atmospheric showers they produce, by means of ground-based detectors, since the fluxes of high-energy photons are low and decrease rapidly with increasing energy. These ground-based detectors should be placed at high altitude, where atmospheric dimming is lower.

1.8.1 Satellites

Satellites HE gamma-rays telescopes such as Fermi-LAT detect the primary photons at energies lower than ground-based telescopes. The geometry of the conversion of an incident photon into an e^+e^- pair in foils of heavy materials which compose the instrument in planes of silicon detector, determine the direction of the incident photon. The Gamma Fermi observatory, launched in June 2008, is composed by the spacecraft and by two instruments: the Large Area Telescope (LAT) and the Fermi Burst Monitor (GBM). The two instruments work as a single observatory. The LAT consists mainly in a tracker, an anti-coincidence apparatus and a calorimeter. Its energy range is 20 MeV-300 GeV, while the energy range explored by GBM goes from 10 KeV to 25 MeV. The effective area of LAT approaches 1 m^2.

1.8.2 Ground-based detectors

Ground-based VHE telescopes detect the secondary particles of the atmospheric showers produced by primary photons and cosmic rays of energy higher than the primaries observed by satellites. They have a huge effective area, so their sensitivity is high. They detect a huge amount of background events. There are to classes of ground-based HE gamma-rays detectors: the Extensive Air Shower arrays (EAS) and the Cherenkov telescopes.

1.8.3 EAS detectors

The EAS detectors, such as MILAGRO and , are made by a large array of detectors sensitive to the charged secondary particles generated by the atmospheric showers. The lower energy threshold of EAS detectors is at best in the 0.5-1 TeV range. The direction of the detected primary particles is computed by taking into account their arrival times, and the angular precision is about 1 degree. Energy resolution is also poor.

1.8.4 Cherenkov Telescopes

Imaging Atmospheric Cherenkov Telescopes (IACTs), such as HESS, VERITAS and MAGIC, detect the Cherenkov photons produced in air by charged, locally superluminal particles in atmospheric showers. They have a low duty cycle and a small FoV, but they have a high sensitivity and a low energy threshold. The Cherenkov light collected by a large optical reflecting surface onto a camera made by an array of photomultiplier tubes, with typical quantum efficiency of about 30%, is projected in the focal plane of the reflector. The camera has a typical diameter of about 1 m, which corresponds to a FoV of 5×5 degrees. The signal collected is analogically transmitted to trigger systems. The events which passed the trigger levels are sent to the data acquisition system, which operates at a frequency typically of a few hundred Hz. The typical resolution on the arrival time of a signal on a photomultiplier is better than 1 ns. Since about 10 photons for square meter arrive in the light pool for a primary photon of 100 GeV, a collector of area 100 m^2 is sufficient to detect gamma-ray showers if placed at mountain-top altitudes. Data can typically be taken only in moonless time, or with moderate moonlight, because of the faintness of the signal. This limits the total observation time to some 1500 hours/year [9].

2 Active Galactic Nuclei

2.1 Introduction

The term "Active Galactic Nuclei", or AGN, refers in general to the existence of energetic phenomena in the central regions, or nuclei, of galaxies which cannot be attributed directly and clearly to stars. The visually most striking property of a galaxy hosting an AGN is the brightness of its nucleus region. In most of the cases the luminosity of the core competes, and often exceeds, the brightness of the rest of the host galaxy, in some cases apparently as much as 10^4 times the luminosity of a typical galaxy, in a volume probably $\ll 1pc$. This radiation can emerge over an extraordinarily broad range of frequencies. Active Galactic Nuclei (AGNs) are among the most powerful sources of electromagnetic radiation in the Universe. They produce enormous luminosities (from 10^{42} to 10^{48} erg s^{-1} in very small volumes (probably $\ll$ 1pc). AGNs emit their power in the overall electromagnetic spectrum, from radio to gamma-rays, forming the so called Spectral Energy Distribution, or SED (Fig. 5), in which different processes inside and outside the active galactic nucleus are present. Multi-wavelength photometry is thus a rich source of information about the AGN nature. One method to extract this information is through SED fitting, which consist in comparing the observed photometric data to a combination of physical models for AGN components. It is customary to perform SED fitting using optimization methods as χ^2-minimization, which defines the best fit as the combination of parameters which models the whole SED showing the minimal χ^2 value. However, this method is statistically correct only under the assumption that the parameters are fully independent from each other and thus have a Gaussian probability distribution. This assumption is a drawback of this method since the parameters describing AGN physics are in most cases highly degenerated. To solve this issue can be used an AGNfitter, a bayesian SED fitting code for AGN that allows an integral calculation of the posterior probability distributions of the model parameters taking into account degeneracies and correlations existing among them. AGNfitter samples the parameter space built by the AGN models parameters using a Markov Chain Monte Carlo method. This consists in a random walk that is biased for regions of higher probability in the parameter space, making the code fast and efficient since no time is lost in non-interesting regions. The dimension of the parameter

space sampled by AGNfitter is constructed by 10 parameters, which rule the modeling of four AGN components: the accretion disk radiation, the nuclear hot dust emission and the radiation emitted by the host galaxy and the star burst regions.

AGNfitter constructs SEDs from existing physical models (Fig. 5) and calculate physical parameters that are interesting to AGN physics, such as relevant integrated luminosities and parameters ruling the physics of the host galaxy, such as age, stellar mass and star formation rate (SFR). Moreover, AGNfitter provides both the marginalized and two-dimensional posterior density functions (PDF) of the parameters listed above. Finally, due to the code's Bayesian methodology, the user is able to take advantage of prior constraints on the parameters' distributions. In this way the information given by the likelihood function can be complemented, calculating robustly posterior probabilities of the parameters.

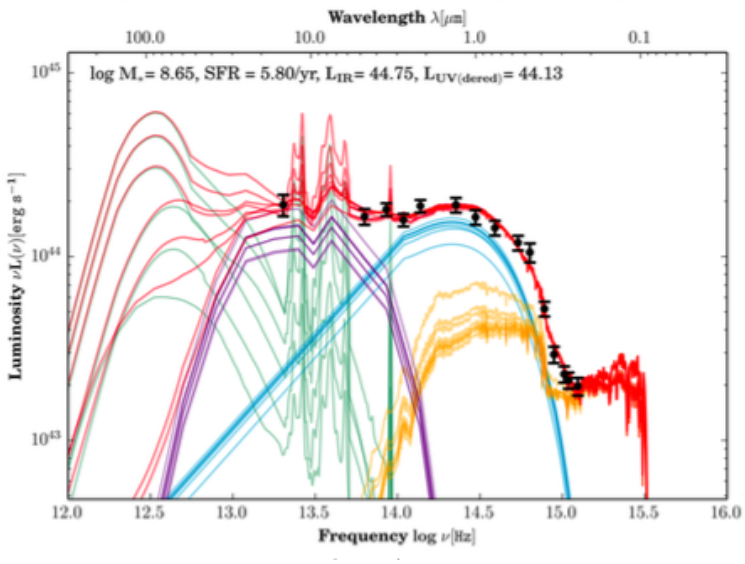

Figure 5: Typical SED of an Active Galactic Nuclei. The green and yellow lines represent the cold dust and galaxy radiation components, while the purple and blue represent the AGN radiation emmited by the hot dust region and the accretion disk respectively.

- *Radio*: radio waves have a nonthermal origin. They are emitted through synchrotron radiation produced by relativistic electrons spiraling in a

magnetic field. Electrons are forced to change direction and, as a result, they are accelerated and radiate electromagnetic energy. The frequency of the emitted radiation depends on the magnetic field strength and on the energy of the electrons. Radio-loud AGNs are powerful radio emitters because relativistic electrons in the jets emit synchrotron radiation. Conversely, radio-quiet AGNs emit weak or null radio waves.

- *Infrared*: the IR band contains reemission from hot dust nearby the active nucleus, that has been heated by the central engine. Therefore, at least around from 1 to 40 μm , the reprocessed nuclear optical/UV/Xray light is dominant. Three pieces of evidence support the thermal origin (Peterson 1997).
  - The 1 μm minimum is a general feature in the SED of AGNs. The IR emission must be thermal since the required temperatures are in the right range (<2000 K) for hot dust in the nuclear regions, while at higher temperatures dust grains sublimate.
  - The IR continuum variability is a probe that the IR originates in dust far away from the central engine heated by the optical/UV radiation. The IR continuum shows the same variations as the optical/UV but with a significant time delay, meaning different distances from the nucleus.
  - The sub-mm break is produced by a rapid decrease in the SED from the far-IR to longer wavelengths.
- *Optical/UV*: the optical band shows emission lines from clouds illuminated by the AGN. Broad emission lines probe regions near the black hole, while narrow lines (FWHM 10^2 km s^{-1}) trace larger-scale outflows. UV radiation comes from thermal plasma at 10^4-10^6 K, generating a superposition of blackbody (BB) spectra that form the Big Blue Bump (BBB).

This excess peaks around 4000 A. Given the high absorption of the Milky Way in the EUV regime ($\nu = 1016$ Hz) the turnover of the BBB is difficult to observe. Around 3000 A there is a small peak, the small blue bump, produced by the blending of Fe II iron lines together with the Balmer lines.

Xray: Xrays (0.1-200 keV) account for 10% of the AGN bolometric luminosity. They can vary rapidly, suggesting an origin in the innermost regions of the active nucleus. The most popular model, invoked to explain

these phenomena, involves accretion onto black holes, i.e. conversion of the gravitational energy of accreting material into electromagnetic radiation, as indipendently argued by Salpeter [42] and Zeldovich [56]. Twenty years later, Rees (1984) [40] theorized this phenomenon involving the accretion of matter onto a Supermassive Black Hole (SMBH), whose mass can be up to 10^9 solar masses. Before accreting, the matter loses its angular momentum and forms a disk around the black hole that emits blackbody (BB) radiation in the UV band. The BB temperature decreases as the distance increases, thus the outer part of the disk, few light days across, emits in the optical regime. The 2-phase model of [19] Haardt & Maraschi (1991) added the corona to this simple representation, in order to produce X-ray photons by Inverse Compton (IC) processes. The corona lies immediately above the disk and it is composed by highly energetic thermal electrons. They boost the optical/UV photons produced by the disk up to X-ray energies. The resulting X-ray spectrum has the shape of a cutoff power law:

$$F(E) \propto E^{-\Gamma(KT,\tau)} e^{-E} \tag{10}$$

Figure 6 shows a schematic diagram of the current paradigm for AGN.

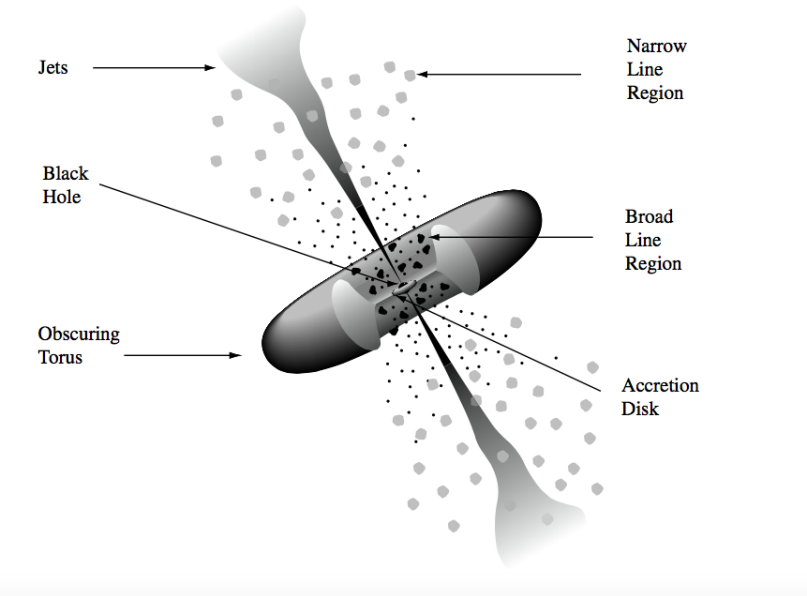

Figure 6: Overview of the diagram

The power law is the composition of many orders of Compton scattering spectra.
A fraction of the photons of the previous scattering order undergoes another scattering amplifying the frequency, until the frequency equals the electron temperature. As photons approach the electron thermal energy, they no longer gain energy from scattering and a sharp rollover appears in the spectrum. Thus the observed high energy spectral cutoff (E_c) yields information about the temperature of the corona.
The relation between the spectral index and the optical depth depends on the geometry of the scattering region. The observed X-ray variability may be caused by variations in the conditions of the corona.

- Gamma-rays: $\gamma-$rays (E>100 MeV) have the smallest wavelength and the greatest energy of any other waveband. In this regime non-thermal processes dominate and it is possible to study the behaviour of some of the most energetic and extreme objects in the Universe.
There are several important mechanisms producing $\gamma-$rays in astrophysical objects. Among them there is the IC scattering (Fig. 7)

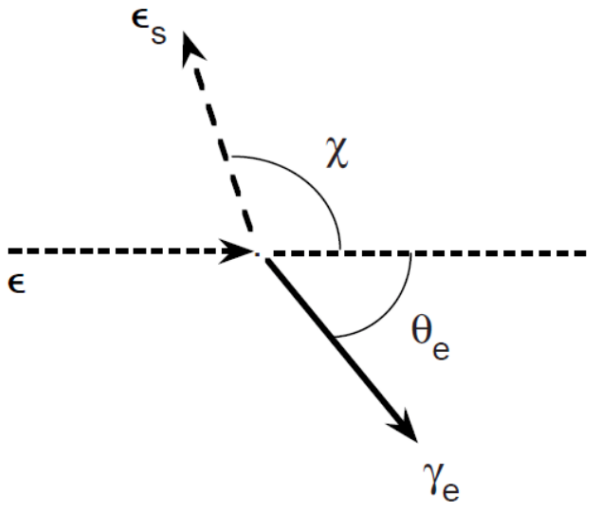

Figure 7: Compton scattering of an incident photon ϵ in the electron rest frame. The photon scatters with energy ϵ_s at angle χ , while the electron is scattered at angle θ_e with lorentz factor γ_e

This process takes place when high-energy relativistic electrons scatter low energy photons to higher energies (e.g. in the jets). The frequency of the up-scattered photons is proportional to

$$\gamma_e c^2 \nu \tag{11}$$

where γ_e is the Lorentz factor of the electron, and ν is the initial photon frequency.
The presence of a black hole at the center of an AGN was long suspected. Most experts believe that the power for an AGN comes from accretion onto a supermassive black hole with a mass from millions to billions of solar masses. The accretion mechanism is widely studied and at the same time widely unknown. A supermassive black hole accretes matter and powers jets (collimated higly relativistic outflows). Many fundamental aspects of AGN jets and of particle acceleration in these jets are poorly understood, including the mechanisms that launch the jets, and their composition. The studies of AGN started in 1908, when E.A. Fath in the Lick Observatory performed his study of the spectra of what were called "spiral nebulae". Most of these

objects showed spectra with absorption lines, that Fath understood as coming from the integrated light of a large number of stars present on these "nebulae". A very small fraction among the total galaxies showed spectra with many high-ionization emission lines, as demonstrated by [43]. Seyfert selected a group of galaxies on the basis of high central surface brightness. Seyfert obtained spectra of these galaxies and found that the optical spectra of several of these galaxies are dominated by high-excitation nuclear emission lines. In his honour, the AGN that show broad emission lines, coming out from a small, bright, and with quasi stellar apparence nucleus, are known as Seyfert galaxies. Seyfert galaxies received no further attention until 1955, when NGC 1068 and NGC 1275 were detected as radio sources. These Seyfert galaxies constitute, as also the quasars, the most common types of AGN.
Afther Second World War there was a development of radio astronomy, that allowed to identify optically strong radio sources. In particular the detected source Cygnus A was identified with a faint galaxy with a redshift $z \approx 0.057$, proving its extragalactic origin. Other similar sources were then found and were called radio galaxies. Some of the earliest radio astronomical observation discovered that many bright radio sources come in the form of double lobes with a galaxy located between them. Many of the known AGNs are strong radio emitters and given the high resolution of radio instruments the phenomenology of that emission is widely studied. M87 is a very interesting example of a radio galaxy detected also at TeV energies. These sources showed spectra of the compact and very luminous cores often rich in emission lines broader than the ones seen in normal galaxies and very similar to those present in Seyfert galaxies. Radio galaxies are in a smaller proportion compared to the Seyfert galaxies. Seyfert galaxies are radio quiet objects. AGN are special laboratories for extreme physics that we would like to understand. They are also our principal probes of the Universe on large scales, so understanding them is essential to study the formation of the Universe.

2.2 Classification of AGN

The population of AGNs can be divided in two big groups, radio loud and radio quiet AGN. Given the numerous different characteristics that an active galactic nucleus may have, a further sub-classification can be done into several sub-groups, each one collecting some of their possible features. The full complement of AGN constitutes a zoo of different names, detection criteria, and spectral, variability and polarization characteristics [51]. Even if their spectra span over all the frequencies, the optical and radio observations of AGNs originate their classification. Figure 8 shows an schematic AGN classification, based in the luminosity, in the morphology, and in the inclination angle with respect to the observer of the host galaxy.
Rougly 5-15% of the Active Galactic Nuclei are radio-loud. The characteristic of radio-loudness may be related to the host galaxy type or to Black Hole spin which is thought to enable the formation of powerful relativistic jets. The so-called unified model explain the main differences of the AGN according to a few characteristics. A supermassive Black Hole with a mass of 10^6 - 10^{10} solar masses is located in the center and it is the the final engine of the AGN. This BH accretes matter forming a disk of hot plasma. The ionization of the gas close to the accretion disk constitutes the Broad Line Region (BLR), named in this way because lines are Doppler-broadened due to the fast motion caused by the proximity to the Black Hole. Farther from the central engine, other clouds with slower motion constitute a region were are observed narrow emission and absorption lines (Narrow Line Region, NRL). The previous regions are finally surrounded by a dust torus in the equatorial plane that obscures all the central region, depending on the viewing angle. A pair of opposite jets of ultra-relativistic moving plasma will emerge from the polar regions of the system, in the case that accretion rates are high enough. Any radiation produced inside the jet is measured modified due to Doppler Effect, as the jet move at relativistic speeds. Large radio lobes are sometimes seen close to the outer end of the jet. The main differences observed in Active Galactic Nuclei could be explained as due to the matter accretion rate, the mass of the central BH, and the viewing angle of the object.
Radio-loud AGN always show jets and they can be divided into the ones where the jet stuck in dense matter or the ones rom where the jet escape, according to the lengths of the jet, developing typical jet length of ≥ 100 kpc. Radio measurements plays an important role, concerning the evidence of rel-

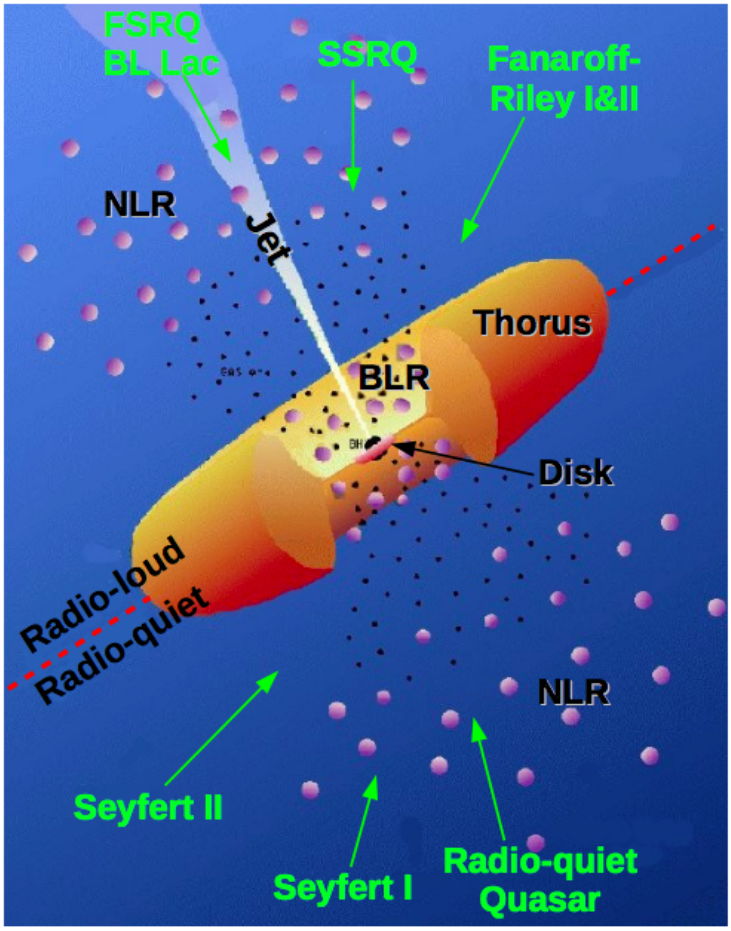

Figure 8: Schematic AGN classification

ativistic beaming. The apparent superluminal motion as also the asymmetry of the giant radio lobes supports the presence of relativistic jets.
The rapid variability at high energy (γ-rays) also supports the relativistic beaming. In fact a maximum size for the emitting region and in order for γ-rays to escape to the source, the optical depth for pair production $\tau_{\gamma\gamma}$ is incompatible with the observed luminosity.
The asymmetry is probably originated by a line of sight close to the jet axis of the Active Galactic Nuclei, leading to a relativistic boosting of the forward jet only. Different orientations of the AGN axis with respect to the observer would explain easily the observed "zoology" of AGNs and it is not necessary to involve different type of object to explain the various typology of phenomenological evidences (see sketch in Figure 9).

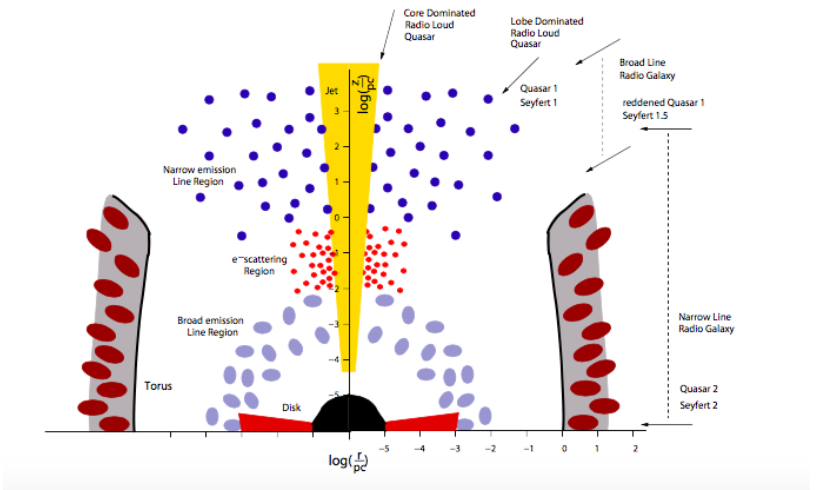

Figure 9: Sketch of different AGN objects

The radio-loud AGN that show developed jets can be further classified according to their luminosity, that is correlated to differences in the morphology of the jets [FR74]. The usual criterion to distinguish "high" and "low" luminosity sources is the radio luminosity at 178 MHz. Objects with $L_{178} \geq 2.5 \times 10^{26}$ W/Hz are highly luminous and show strong jets that extend far outside the host galaxy. The jet luminosity is increased at the outer regions, showing extended radio lobes and hot spots. These objects are further divided in FSRQ, SSRQ and Fanaroff-Riley II (FRII) radio galaxy types. Object with $L_{178} < 2.5 \times 10^{26}$ W/Hz show jets fainter than in the previous, more luminous AGN, and a luminosity decrease at larger distance from the central engine. In this case the jet does not show hot spots. These object are further divided in BL Lac objects and in Fanaroff-Riley I (FRI) radio galaxy types. If the observation angle of the jet is large, the inner part of the AGN are obscured by the torus, and therefore the thermal continuum radiation from the disk and the broad line region are shielded. In this case, the AGN is classified as radio galaxy.
Figure 10 shows a X-ray, radio and optical composite image of a typical radio galaxy.

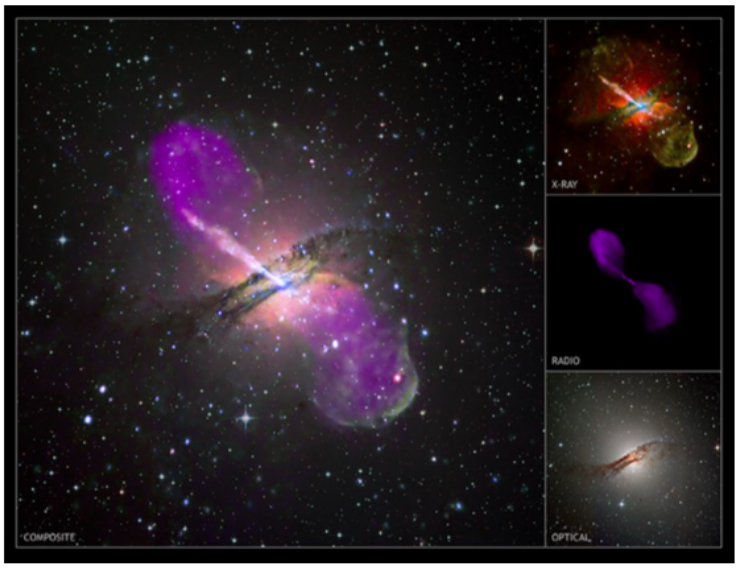

Figure 10: A Chandra image composite with optical and radio data, of the nearby FR-I radio galaxy Centaurus A, providing a view of the two opposite jets coming from the central super massive BH, extending to the outer reaches of the galaxy. At the end of each jet an extended radio lobe is present. This source has been confirmed as a VHE gamma-ray emitter by the H.E.S.S. array. (Credit: X-ray: NASA/CXC/CfA/R.Kraft et al; Radio: NSF/VLA/Univ.Hertfordshire/M.Hardcastle; Optical: ESO/WFI/M.Rejkuba et al.) from http://chandra.harvard.edu

For very small inclination angles ($< 12^\circ$), the jet points toward the observer. In this case the radiation from the AGN is dominated by the radiation from the jet, since the bulk motion of the jet is relativistic, with the effect of greatly increased of the luminosity from the jet radiation. These AGN which present a strong beamed emission, show a flat radio spectrum, with a highly variable flux, and polarized radiation. The AGN that fit in this description are commonly grouped in the term "blazars" (BL Lac objects and FSRQ). The BL Lac objects are less luminous objects that show a FRI-type jet and almost no emission line, while the FSRQ are high luminous objects that show a FRII-type jet and strong emission lines. The emission from blazars is often shown in Spectral Energy Distribution (SED) plots. Their SEDs have a two-bump structure (see Figure 11).

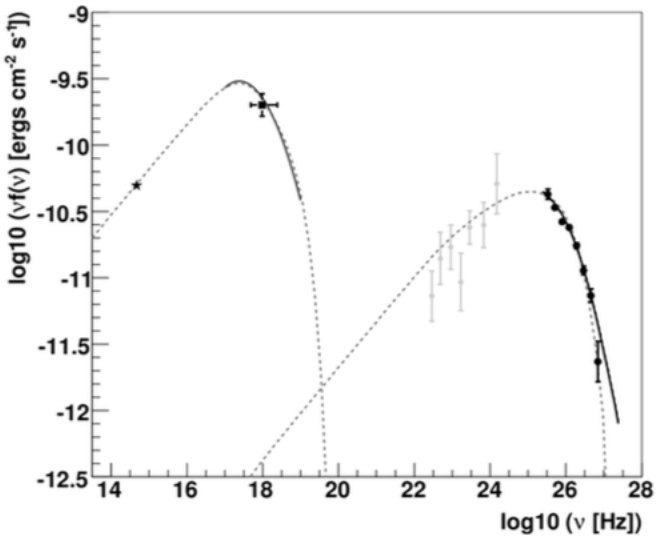

Figure 11: Example of the SED of Mrk 421, a VHE gamma-ray emitter blazar, as measured in 2004-2005 by various instruments

The high energy peack of the SED of blazars is normally located at the MeV-GeV range.

2.3 Blazars

We can define blazars as the AGNs with one of their jets pointing straight to the observer or as the AGNs characterized by fast variability, γ-ray emission, none or dimmed emission lines. The main characteristic of the blazars is their non-thermal beamed continuum emission, because of the plasma moving at relativistic speeds, along directions close to the line of sigh.
Blazars are strong radio emitters, and compact sources.
Blazars are also divided in two sub-classes: Flat Spectrum Radio Quasar (FSRQ) and BL Lac objects.
The key element of blazar emission is the relativistic jet. To explain the observed broad-band spectrum most model assumes that there is an acceleration within the jet of a relativistic population of particles (electrons, protons, or both).
A very important role in the emission properties of these objects is played by the relativistic beaming.
Blazars are bright in all wavelenghts and they exhibit strong flux variability (from minutes to years time scales) in all observed energy band. Many blazars are also strong γ-ray emitters, also in the VHE band. The low energy component of their SED is attributed to electron synchrotron emission, while the origin of the high energy component is still debated intra "leptonic" and "hadronic" scenarios of models.
In 1998 Fossati et al. [12] published a study about the property of the SED of a large sample of blazars. What they found about their SED structure can be summarized in the three following point.

- The first peack occurs in different frequency ranges, with most luminous sources peacking at lower frequencies.
- The peack frequency of the high-energy bump correlates with the peack frequency of the low-energy one.
- The luminosity ratio between the high and the low energy components increases with bolometric luminosity.

This is the so-called "blazars sequence" visually described in Figure 12.

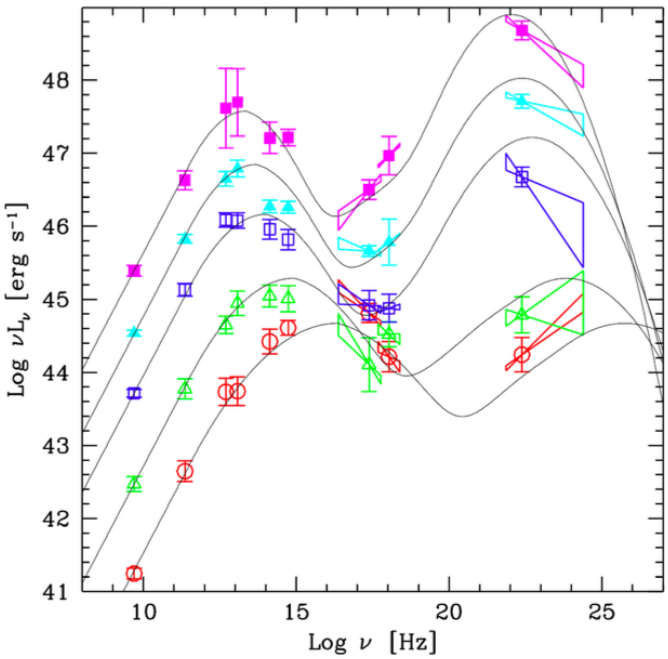

Figure 12: The average SED of blazars, which shows a distinct double peak for all sources, widely attributed to the synchrotron and inverse Compton processes. The apparent anti-correlation between the low energy synchrotron peak and the bolometric luminosity has historically been referred to as the blazar sequence.

This scheme is popular because a single parameter, related to the blazar luminosity, would govern the radiation mechanisms and the physical properties in the relativistic jet present in FSRQs as well as in BL Lac objects, but is a very difficult task to obtaining unbiased samples of blazars and to consider all the possible selection effects which might result in the observed properties and correlations.
The γ-ray data collected by the Fermi telescope may sheld more light on the blazars sequence.
Blazars can be observed almost in the full electromagnetic spectrum, along about 20 decades of energy. At the high energies blazars are the most energetic types of AGN. Their luminosity would be as high s $L_\gamma = 10^{49}$ ergs/s, assuming an isotropic emission. An assumption of a beamed emission with a beaming factor of 10^{-3} would still mean a very high luminosity of $L_\gamma = 10^{46}$

ergs/s.
The origin of the energy that powers the system is the central BH, as stated before. It is not obvious however how the energy can be extracted from the BH and why should it appear as a relativistic jet. The formation of a jet is a phenomenon often seen in astrophysics. The term "jet" was first used in extragalactic astronomy by Baade & Minkowski (1954) [4] to describe the optical linear feature in M87.
It is understood that the energy needed to create the jets is coming from the rotational energy of the BH, even if the main source of the energy of the AGN is the gravitational energy of the central massive BH. The rotational energy would come either from the merging of two Black Holes, or from a residual angular momentum from the original cloud of gas that created the BH, by accretion of extragalactic material. To explain the jets formation many different models are proposed: models that involve thermal pressure of the accreting gas and the relativistic effects of a rotating Black Hole or models that involve a rotating charged Black Hole.
The relativistic nature of the jets is evidenced by the observed synchrotron emission by relativistic electrons, that give origin to the low energy emission peak in the SED. Others evidences of the relativistic nature are the apparent superluminal motion of knots in the jets, the presence of highly variable polarization in both optical and radio emission, and the VHE observations.

2.4 Radio galaxies

A radio-loud galaxy is a particular type of active galaxy that emits more light at radio wavelengths than at visible wavelengths. Radio galaxies are driven by non-thermal emission. Observations from radio telescopes showed that some radio galaxies, called extended radio galaxies present

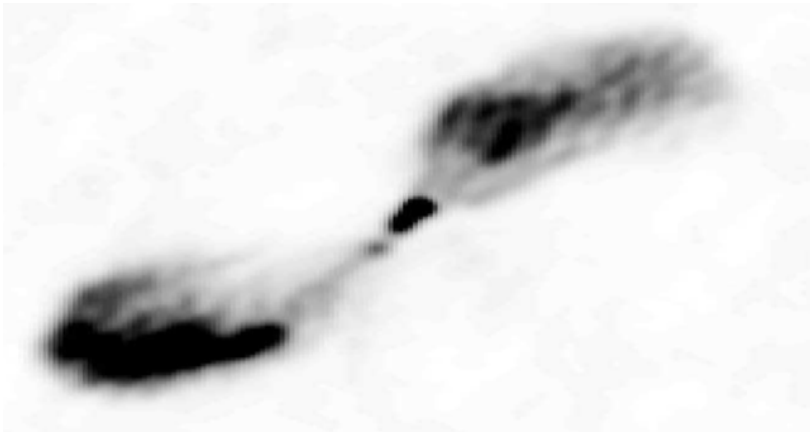

Figure 13: A typical radio image at 21 cm of the FR I radio galaxy Centaurus A

The main structural components of a radio source are (see Fig. 13):

- The *core*: compact region with flat radio spectrum (α of the order of zero. It is still very difficult resolve the central region even with a 10 mas VLBI resolution.

- The *jets*: collimated outflows of relativistic plasma that originate in the central region of the AGN and reach kpc or even Mpc distances. In the radio band jets emit synchrotron radiation, and the resultant spectrum is a power law,

$$S_\nu \propto \nu^{-\alpha} \tag{12}$$

  with $\alpha = 0.6$ ([32]). Jets are also visible in the optical and X-ray bands [20]. At high energies the involved physical processes are synchrotron or inverse Compton.

- The *hot-spots*: bright compact regions located at the end of the jets. They are produced when the jet impacts the ISM generating shocks. The X-ray emission from the hot-spots of several radio sources, for example Cygnus A, conform to a Synchrotron Self-Compton (SSC) model with a magnetic field close to equipartition 1 (Wilson et al. 2001). However in other cases, for example Pictor A, the X-ray emission cannot be explained by the SSC model.

- The *lobes*: extended structures lying in opposite directions, reaching even Mpc distances from the nucleus. They are filled with plasma passed along the jet and through the hot-spots. The radiation emitted by lobes has non-thermal origin. Specifically, the radio emission is due to synchrotron, while in the X-ray band the emission process is usually Inverse Compton scattering of the microwave background radiation. Recentlyγ-ray emission from the lobes of the radio galaxy Centaurus A has been discovered by the Fermi collaboration.

The total energy in a single radio lobe is about 10^{53} J. As a comparison, a typical supernova explosion puts out approximately 10^{44} J of energy.
According to the unified theory, these radio lobes are the ends of jets produced by a supermassive black hole at the center of the galaxy. The jets extend on each side of the galaxy perpendicular to the central accretion disk

which surrounds the BH because it is easier for the jet to move perpendicular to the disk (where there is not much material) than through the thick disk. This is why we see two jets moving in opposite directions.
As they travel through the intergalactic medium, these jets may become twisted by the motion of the galaxy itself or even be made to change direction due to the streaming motions of the medium. These effects make each double-lobed radio galaxy unique and interesting.
Figure 14 show an HST picture of a typical radio lobed galaxy.
Radio galaxies have been historically classified by [11] in FR type I and II, depending on their extended radio morphology that changes over, or under, a critical radio power at 178 MHz, $P_{178MHz} = 10^{25}$ W Hz^{-1} sr^{-1}.

- FRI are weak radio sources, characterized by turbulent decelerating jets and kpc scale relaxed lobes. Their host galaxies are generally brighter than those of FRIIs, and are usually found at the centre of clusters (Prestage & Peacock 1988) and have a dominant cD morphology. Their optical spectra show weak emission lines. The minimum energy or equipartition is given when the energies are nearly equally distributed between relativistic particles and the magnetic field.

- FRII or classical double are bright radio sources with relativistic jets, edge-brightened lobes and bright hot-spots far from the nucleus. FRII hosts are generally isolated ([39]) and avoid cD galaxies. Their optical spectra usually show strong emission lines.

Two accredited hypothesis try to explain the different radio morphology of FRIs and FRIIs.

1. The interplay between the jet energy and the density of the environment; in this scenario FRIs and FRIIs are different manifestations of the same phenomenon.

2. Different accretion modes onto the SMBH; for FRIIs a standard ([44]) radiatively efficient accretion disk is invoked, instead for FRIs low accretion rates and low radiation efficiencies are proposed. The transition from FRIs to FRIIs would be due to a change in the accretion mode and can be related to an evolutionary scenario [14]. It is possible that all AGNs pass through a jet phase (FRII), then when the accreted gas is exhausted the AGN turns into lowpower FRIIs and successively FRIs.

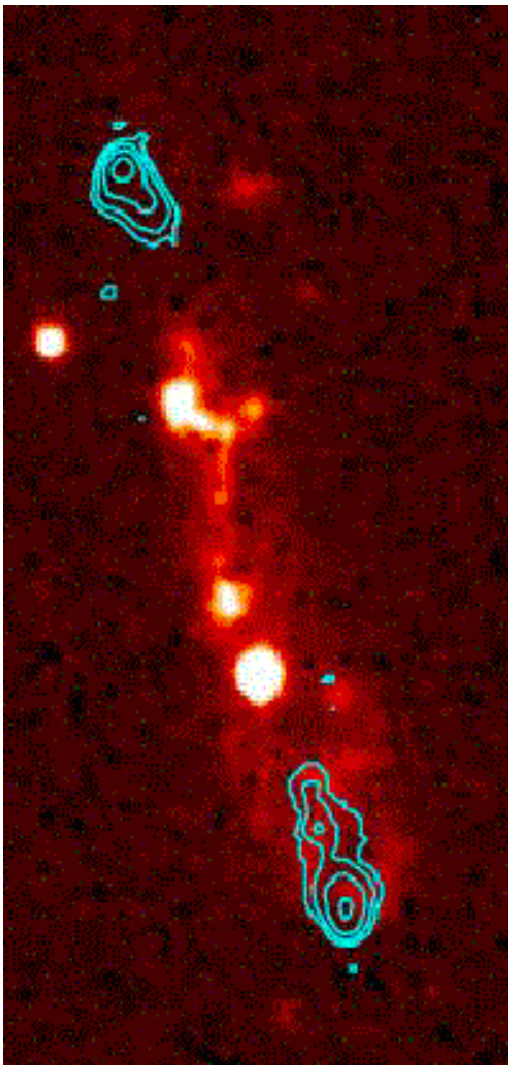

Figure 14: image of a typical radio lobed galaxy

A recent review, divides radio galaxies in thermal and non-thermal sources depending on their accretion modes. Thermal Radio Galaxies contain hidden (by the torus) quasar nuclei, while non-thermal ones are weakly accreting galaxies (but powerful synchrotron emitters) characterized by weak low-ionization lines. Besides FRIs and FRIIs, there is also another class of objects, the Compact Sources, that are powerful radio emitters peaking at MHz-GHz frequencies. They are very small, generally in the size range 1-20 kpc, i.e., smaller than typical host galaxies. To date there are two possible explanations for their compactness:

1. they are young AGNs in expansion through interactions with the ISM, and this is supported by estimates on the jets ages around $10^4 - 10^6$ yr through VLBI proper motions [17];

2. they are frustated AGNs confined by the ISM and so not evolved in full-size AGNs. However, this latter scenario is less plausible since the densities and properties of the surrounding gas are comparable with those in extended AGNs [35].

There are two main types of compact sources: the Compact Steep-Spectrum (CSS) sources and the Gigahertz Peaked Spectrum (GPS) sources. CSS are miniature classical double radio galaxies with more pronounced asymmetries. They are extended on kpc scales with an estimated age around 106 yr and have steep spectra ($\alpha > 0.5$). GPS are powerful radio sources, peaking at GHz frequencies (smaller galaxies peak at higher frequencies). They are smaller than CSS, in fact their extension is contained within the NLR (1 pc). Finally, RL quasars are subdivided into two different groups depending if they are steep radio spectrum dominated (SSRQs, $\alpha_r > 0.5$) or flat radio spectrum dominated (FSRQs, $\alpha_r < 0.5$). SSRQs tend to have lobe-dominated radio morphologies, while FSRQs often have coredominated radio structures and are highly variable.

2.5 MeV/GeV emitters

MeV blazars have quite steep spectra beyond MeV energies (with photon index greater than 2), in contrast to the so-called GeV blazars with flat gamma-ray spectra extending to GeV energies. But, most probably, there is no fundamental difference between MeV and GeV blazars. It is believed that both classes represent the same AGN population flat spectrum radio quasars (FSRQs). The difference between MeV and GeV blazars can be explained within the so-called external Compton model, assuming that GeV flat spectra originate in the broad emission line (BEL) regions, where their production is dominated by Comptonization of optical-UV emission lines, whereas the spectra of MeV blazars are formed at distances where the target photons are supplied by hot dust. Moreover, it is possible that the MeV and GeV blazar phenomena can appear interchangeably within the same object like in PKS 0208-512 [46].

2.6 Gamma-ray emission models

Emission models are generally divided in two big categories, depending on the nature of the particles that are accelerated (electrons and positrons or positrons, respectively): "leptonic" and "hadronic". Different channels have been proposed: interaction of protons with magnetic fields (synchrotron radiation), IC scattering of electrons, photon fields (photon-meson processes) and matter (inelastic p-p collisions). Phenomenological models frequently leave open the question of how the particles are accelerated: by centrifugal acceleration of particles along rotating magnetic field lines near the base of the jet, by shock-wave acceleration in MHD (Magnetic Hydro-Dinamics) turbulence in the jet, or by shear.

2.7 SED

One of the defining characteristics among radio loud AGN, and in particular among the gamma-ray blazars, are the broad, double-peaked spectral energy distributions (SEDs) in the representation of their broadband emission.
As it was said in section 2.3, blazars show a two bump structure in their SED, that is understood to originate by emission from the electrons from the jet, spiraling at relativistic velocities in the magnetic field lines of the jet. The low energy component of the SED is attributed to electron synchrotron

emission. The high energy component origin is still debated, but is most commonly attributed to IC emission. Within the blazar subclass of AGN, Fossati et al. (1998) found that there existed a negative correlation between the peak position of the synchrotron component and the intrinsic synchrotron peak luminosity, which Donato et al. [10] found could be described fully using a single parameter, namely the bolometric luminosity. In addition, it was found that the dominance of the gamma-ray peak became more pronounced with decreasing synchrotron peak frequency. These correlations were referred to as the blazar sequence, and led Ghisellini et al. to suggest that the correlation was intrinsically tied to the blazars, due to the decreasing intrinsic power of the source being coupled with decreasing cooling effects from a reduced external radiation field as the peak frequency moved from low to high frequency. Specifically, in luminous blazars with high photon energy densities due to accretion disk and line emission, the synchrotron radiating electrons lose energy through Compton up-scattering, producing strong gamma-ray components and lower synchrotron peak frequencies, while the electron energy distribution remains hard in less luminous BL Lac objects, which lack strong line emission, producing high-frequency synchrotron peaks and low gamma-ray luminosities. Thus the blazar sequence can be explained naturally.

Following these initial results of the blazar sequence, evidence against the blazar sequence has been mounting, as the number of known blazars has increased, and it has been found that the previously observed correlation does not fully describe the newer data sets. Furthermore, Nieppola et al. (2008) [33] argued that the negative correlation between synchrotron peak frequency and bolometric luminosity could in fact be due to an observational effect that arises from a negative correlation that they measured between the source luminosity and the Doppler factor, which had been ignored in previous work. While the diversity among blazars may not allow such a simple description as the blazar sequence implies, much of the terminology in terms of the SED classification remains a useful tool, as there nevertheless remains a number of observational properties that can be correlated with the location of the synchrotron peak among the FSRQ blazars and BL Lacs. In particular, the SED classification of low synchrotron peaked (LSP), intermediate synchrotron peaked (ISP), and high synchrotron peaked (HSP) blazars originally established to classify BL Lac objects is still used within the literature, and has also been carried over in some cases to the blazar population as a whole. In particular, sources are classified as LSP if their synchrotron peak

ν <1014 Hz, while ISP peak sources have 1014 Hz $< \nu <$ 1015 Hz, and HSP sources have $\nu >$ 1015 Hz. Among the gamma-ray blazars, the diversity in ν is most widely noted within the BL peak Lac population, with a relatively even distribution of sources across the frequency range 1013 Hz $< \nu <$ 1015 Hz, while the FSRQ blazars are almost exclusively LSP sources, although some ISP FSRQs have been found.Another important relationship that still holds for the vast majority of blazar sources is that of the ratio between the synchrotron and IC peaks for each of the subclasses. In particular, the FSRQ and LSP BL Lac populations are characterized by soft gamma-ray photon indices, with their IC peaks occurring at or near 100MeV. HSP sources, on the other hand, are characterized by much harder spectral indices (and, in general, lower bolometric luminosities, in agreement with the blazar sequence), with IC components that peak at or above 10GeV. This is in some sense not surprising, given the underlying synchrotron self-Compton (SSC) and external Compton (EC) processes that appear to be at work in the vast majority of these objects.
Figure 15 show the spectral energy distributions of 2214 blazars sorted into five bins of radio luminosity.

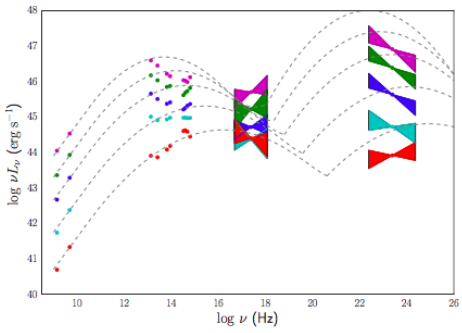

Figure 15: Spectral energy distributions of 2214 blazars sorted into five bins of radio luminosity (purple, red, green, cyan, and blue, in order of decreasing luminosity at 1.4 GHz); the anti-correlation of synchrotron peak with luminosity is visible, although a big blue bump (at high luminosities) and host galaxy emission (in the lowest luminosity bin) are comparable to the synchrotron contribution. The analytic form SED proposed by Fossati et al. (1998) based on 126 blazars (dashed lines) clearly does not fit the more extensive data, in Mao et al., 2016, arxiv:1603856v1

2.8 Correlations

It is useful to observe the activity of blazars simultaneously or quasi-simultaneous in different energy ranges, in order to understand the nature of an AGN. Several satellites provide full-sky monitoring data for the X-ray and the γ-ray range. Also the optical band is pretty well covered given the numerous optical telescopes operating around the world. Pointing observations can be also scheduled in all the interesting energy bands (radio, UV, X-rays, etc.) but the time granted depends on the avaibility of the single instrument.
From study of the lightcurves of the source one can extract possible correlations in the flux variations within the different frequency ranges or the typical variability of the source.

3 Radio-Gamma connection

3.1 Introduction

The extragalactic gamma-ray sky is largely dominated by radio-loud active galactic nuclei (AGN). In particular, the population of blazars represents almost 97 % of the gamma-ray emitting AGN from the 2LAC catalogue.
Blazars, the most extreme class of Active Galactic Nuclei (AGNs), are observed at almost the full electromagnetic spectrum from radio to γ-ray band. It contains two subclasses called BL Lacertae objects (BL Lacs) and Flat Spectrum Radio Quasars (FSRQs).
The high energy emission is likely due to inverse Compton scattering off the low energy photons by the relativistic electrons which are also responsible for the synchrotron emission observed in the radio band.
A connection between the radio and gamma-ray emission in blazars has long been suspected, and has received renewed attention during the era of the Fermi Large Area Telescope (LAT) [13].
It is straightforward to demonstrate a statistically significant correlation between observed gamma-ray and radio luminosities or flux densities, as was done during the era of the EGRET instrument. However, because of distance effects, Malmquist bias, and the strong variability exhibited in blazars, such an apparent correlation may or may not correspond to an interesting intrinsic correlation. Recent studies using LAT data and concurrent or nearly concurrent radio data provide strong evidence for an intrinsic correlation [26]. The data concurrency reduces or eliminates spurious effects from variability, and Monte Carlo statistical methods demonstrate that the correlation is not due to other biases.
Although in blazars all the ingredients needed for this scenario are present, a clear connection between the emission at the edges of the multiwavelength spectrum has not been unambiguously established yet. In particular, the trigger of the high-energy flares typically observed in blazars, and the location of the gamma-ray emitting region are still uncertain. Thanks to their luminosity variability observed throughout the electromagnetic spectrum, we have a chance to shed a light on this issue. The variability behaviour shown in the various energy bands (i.e. time-delay, duration, intensity) provides us tight constraints on the location and size of the gamma-ray emitting region. For example, intra-day variability is an indication of a very compact region. Moreover, a time delay in the emergence of the flare at progressively longer

wavelengths may locate the high-energy emitting region in the innermost part of the AGN where severe opacity effects play a role.
On the other hand, the detection of gamma-ray and millimeter-wavelength flares occurring almost simultaneously may indicate that the high-energy photons are produced much further out, downstream along the jet. High-resolution observations performed with the Very Long Baseline Array (VLBA) found that superluminal jet components are ejected close in time with strong gamma-ray flares.
With the aim of understanding the origin of gamma-ray emission, multi-wavelength monitoring campaigns triggered by strong high-energy flares are required. Thanks to the high sensitivity and the gamma-ray all-sky monitoring, the Large Area Telescope (LAT) on board Fermi has proved to be a superb hunter of gamma-ray flares. However, despite the efforts a clear picture is far from being drawn. From the detailed study of the most variable sources it seems that not all the flares have the same characteristics, even if produced within the same source.
The connection between radio and γ-ray emission can help us constrain the radiation process and the emission region in the jets, especially for the γ-ray band. This has been considered since the era, but no confirmed conclusion had been made due to the limits of the sensitivity of the telescope and the erratic sample [26]. Thanks to the high sensitivity, broad energy range, and large view field of Large Area Telescope (LAT, [3]) on board the Fermi Gamma Ray Space Telescope (Fermi) launched successfully in 2008, much larger sample and more accurate photon flux and spectrum have been achieved.
After two years of survey of the LAT, the second LAT AGN catalog (2LAC) gives a more accurate classification and association of 1121 AGNs in γ-rays, and 886 sources in its clean sample. Some radio monitor programs are processing in Fermi era at different frequency, e.g., MOJAVE (Monitor of Jets in AGN with VLBA Equipment) program at 15GHz, the OVRO (Owens Valley Radio Observation) program at 15GHz, UMRAO (the University of Michigan Radio Variability Program) at 4.8, 8.0, and 14.5GHz, and so on. These programs give us a good chance for investigating the connection between radio and γ-ray emission with quasi-simultaneous data.
Radio observations present a rich phenomenology in studies of AGN extensive multifrequency lightcurves, observations and statistics of superluminal motions, radio spectral polarimetric imaging on all scales (jets, hotspots, lobes), and an abundant variety of source types including young radio sources

and radio-quiet objects. In the EGRET era, there were 66 high-confidence blazars identified with gamma-ray sources (27 lower-confidence) and only a few radio galaxies (e.g., Cen A, 3C 111). Now we are in the era of the Fermi Gamma-ray Space Telescope with the increased capabilities provided by the Large Area Telescope (LAT). The 2nd LAC AGN catalog (2LAC) clean sample included: 310 flat spectrum radio quasars (FSRQs), 395 BL Lacs, 156 blazars of unknown type, and 24 AGNs (include radio galaxies). FSRQs have been detected with $L_\gamma = 10^{48}$ erg/s up to z=3. For Cheung (2012) [7] significant correlations are present between radio and gamma-ray properties. FSRQs are on average brighter and apparently more luminous in the radio band than BL Lacs (but a redshift incompleteness is present). Thanks to the 1st Fermi-LAT Hard source Catalog (1FHL) which includes data from August 2008 through July 2011, possibly softer AGN gamma-ray spectra appear with increasing redshift, and many new targets are now available for current and future TeV telescopes. The high energy emission site for AGN can be probed with gamma-ray imaging in exceptional cases, like in the giant radio lobes of Centaurus A (and possibly in NGC 6251, and Fornax A). Moreover Fermi detected giant gamma-ray bubbles in our Galaxy (5.4) and a possible young radio source (4C+55.17). In the coming years, it will be possible to extend the radio/gamma-ray correlations to low fluxes/luminosities, to continue to identify possible sites of gamma-ray emission, to test if radio-quiet AGN are also gamma-ray quiet, and to look for bubble sources in nearby galaxies.

Radio-loud systems appear to be the only AGN loud in gamma-rays. In addition to blazars and radio galaxies, the only newly established class of gamma-loud AGN are the radio-loud narrow line Seyfert 1s (NLS1s). Radio-quiet Seyferts seem gamma-quiet as well. Radio properties of nuclear jets may be directly related to gamma-ray properties. However, nuclear relativistic jets are not the only relevant gamma-ray production site as lobes and bubbles are observed in gamma-rays. For Stawarz (2012) [48] correlations between radio and gamma-ray properties seem to be present, but more data and better statistics are necessary to understand if they are real or not. In flux-flux limited samples, artificial correlations are expected. Evidence of co-spatiality is not firmly established.

At present, 53 firmly known very high energy (VHE$>$ 0.1 TeV) AGN have been observed. Among them we have 47 blazars, 4 radio galaxies and 1 AGN of unknown type and possibly Sgr A*. The blazar sample includes: 34 high-frequency peaked BL Lacs (HBL), 4 intermediate-frequency peaked

BL Lacs (IBL), 4 low-frequency peaked BL Lacs (LBL), 3 FSRQ, and 2 BL Lacs. The four radio galaxies are: M87, Cen A, NGC 1275, IC 130. Most of them are beamed sources with a strong Doppler boosting as expected since it helps to accommodate fast variability and to avoid strong intrinsic absorption. Variability time scales are from a few minutes to months and years. For Sol (2012) [47] multi-zone synchrotron self-Compton (SSC) models can reproduce most of HBL stationary state spectra.
In 2008, the first NLS1 PMN J0948+0022 was detected by the Fermi-LAT. After that another four NLS1s were detected in gamma-rays. These results confirm the presence of relativistic jets also in NLS1s even though these sources are typically thought to be hosted in spiral galaxies. Their average spectral energy distributions (SED_s) are similar to $FSRQ_s$, but at lower luminosity. SBS 0846+513 is a new gamma-ray NLS1 clearly detected during the third year of Fermi operation, in particular during a flaring state in 2011 June-July. The gamma-ray peak on daily timescale corresponds to an isotropic luminosity of about $10^{48} ergs^{-1}$, comparable to that of luminous $FSRQ_s$. While the kpc- scale structure is unresolved in VLA images, there is a core-jet structure seen in VLBA images. The mechanism at work for producing a relativistic jet in $NLS1_s$ is not clear. Fundamental parameters should be the BH mass and the BH spin. For D'Ammando (2012 [8] this source could be a blazar with a BH mass at the low end of the blazars BH mass distribution. Gamma-ray $NLS1_s$ have larger masses with respect to the entire sample of $NLS1_s$. Moreover prolonged accretion episodes could spin-up the SMBH leading to a relativistic jet formation.
Based on studies using EGRET and the early Fermi-LAT AGN samples, gamma-ray detected AGN were found to show on average faster apparent speeds with respect to other AGN not detected in gamma-rays. To confirm and investigate this, the very long baseline interferometry (VLBI) proper motion results for 198 QSOs and 33 BL Lacs from the Caltech Jodrell Bank Flat-spectrum (CJF) 5 GHz VLBI survey were analyzed. Among these 61 sources have been detected by Fermi-LAT, consisting of 32 FSRQs, 24 BL Lacs, and 5 radio galaxies. For Karouzos [25] conclusions are:

- no strong link is present between fast jets and gamma-ray detection;
- AGN class and gamma-ray variability are connected to jet speeds;
- a correlation between gamma-ray luminosity and apparent velocity is found (higher velocity for stronger gamma-variable sources);

- gamma-ray detected sources appear wider and with larger jet distortions.

Different findings with respect to the previous studies may be due to different observing frequency (probing either different jet regions or structures) or the difference in sampling of the proper motion data.
Blazar studies suffer heavy sample selection effects: e.g., obscuration in optical and X-ray; spectral contamination from accretion disk emission and from lobe (unbeamed) emission; non simultaneous observations; and more. To address blazar sample biases it is important to concentrate on uncontaminated bands. The Fermi 2LAC AGN catalog has no contamination from the host galaxy, even if may still be incomplete due to issues with source associations. The MOJAVE VLBA program provides regular observations of radio-bright AGNs at 15 GHz. With 24 hrs observing sessions every 3 weeks, it assures continuous time baseline data on many sources back to 1994. Among the main results they quote: the brightest gamma-ray and radio-selected quasars have similar redshift distributions; gamma-ray selected blazars have an additional sub-population of low-redshift HSP BL Lacs that are intrinsically very bright in gamma-rays; lowest luminosity BL Lacs (HSPs) all have high gamma-ray loudness (due to SED peak location). For Lister (2012) [27] in BL Lacs (HSP and LSP) the photon index is well correlated with the Compton peak location. This trend could not exist if the gamma-ray and pc scale radio jet emission were fully independent. Analyzing kinematics of 889 discrete features in 201 jets from 1994 to 2011, they derive that: jets of HSP BL Lacs are characterized by lack of compact superluminal features; BL Lac jets have lower radio synchrotron luminosity and lower speeds.
3C 66A is a low frequency peaked BL Lac object at z = 0.444. It is characterized by prominent variability at radio, IR, and optical frequencies. It shows a one-sided core-jet structure with detected superluminal motion. The core shift with frequency has been estimated in 2001 and 2006. A large difference has been found between the two measurements possibly due to a strong flux density increase at 15 GHz in 2006. For Shen (2012) [45] this radio flare is possibly due to the core activity as shown by a new component that emerged from the central core region. Because of their small angular distance in the plane of the sky, 3C 66A and the radio galaxy 3C 66B, are an ideal pair to obtain a combined core-shift measurement of the two sources. Comparison with data at different epochs is confusing: the difference in core shift result cannot be simply explained by the core flare activity. Other parameters apart

from core flux variability may influence the core shift.
A peculiar object to investigate the connection between radio and gamma-rays is the extraordinary case of the flaring blazar PKS 1510-089. The FSRQ, PKS 1510-089 (z = 0.361), shows strong variability and highly superluminal jet components found close in time with gamma-ray flares. Moreover, it was detected at VHE gamma-rays, shows a high level of polarized emission, and a large rotation of the electric vector position angle (EVPA) close in time with a gamma-ray flare. PKS 1510-089 underwent a very active period in 2011 reaching its historical maximum flux density in October 2011. The gamma-ray flare in July 2011 occurred after a rotation of 380 degree of the optical EVPA suggesting a common region for the optical and gamma-ray emission. The new jet component is likely evidence of a shock propagating downstream along the jet. For Orienti (2013) [37] if the gamma-ray flare in October 2011 is related to the radio outburst, it would strongly support the idea that some gamma-ray flares are produced parsecs aways from the nucleus. Note that not all flares have the same characteristics, suggesting shocks with different properties. Follow-up in the mm regime with a high sensitivity VLBI array including ALMA will be crucial in determining the high-energy emitting region.
Blazars show variability on timescale of days suggesting a parsec scale emission region. Comparing the radio-gamma variability, there is evidence that this active region should be inside the broad line region (BLR). Moreover, in some sources the GeV emission shows spectral breaks that could be due to absorption effects inside the BLR. In this context, a relevant case to consider is that of PKS 1222+216 (4C+21.35) which doubled its TeV flux on a timescale on the order of 10 minutes. In this source the location of the VHE emission inside the BLR is problematic because the too strong absorption expected due to the huge optical depth of the BLR. Possibilities to reconcile rapid variability in regions at large distances from the core (outside the BLR) require the presence of jet substructure. Many models have been proposed but not all problems are solved e.g., the presence of mini-jets from fast reconnection in a highly magnetized jet, or narrow electron beams from magnetocentrifugal acceleration, beams from relativistic reconnection, or ultra-high energy (UHE) neutral beams. In conclusion, for Tavecchio (2012) [49] rapid variability is perhaps currently the most compelling issue in high-energy astrophysics. The idea of a unique, large, relaxed emission region is, at least sometimes, inadequate.
On the other hand if the region emitting at VHE is close to the black hole -

accretion disk region (i.e., it is inside the BLR), we expect that gamma-ray flares precede radio variations (assuming as VLBI zero epoch the beginning of a millimeter flare), and little or no correlation with radio variations. If the VHE region is distant, at or downstream of the radio core (i.e. outside the BLR), we expect gamma-ray flares simultaneous, or after, the beginning of radio variations and a correlation between VHE and radio variations. For Valtaoja (2012) [52] comparing data from Fermi and the Metsahovi radio sample, the case for distant gamma-ray origin appears much stronger. Direct observational evidence for close origin was not found; observations point towards distant origins: in the radio-gamma correlations, there are evident delays from radio to gamma. A confirmation of this result will be possible from the final Planck data to model the radio to gamma-ray SEDs with unprecedented accuracy.

It is crucial to understand what sets the maximum power of jets, if jets are powered by black holes (BH_s) or inner regions of the accretion disks. Jet power depends on magnetic field topology: dipolar geometry gives powerful jets, quadripolar or toroidal gives weak or no jets. Jet power increases with increasing BH magnetic flux. BH and a large magnetic flux give a magnetically-arrested accretion (MAD): the BH is saturated with flux, and the B-field is as strong as gravity. Radio-loud AGN have MAD_s with BH spins (a) near to 1 and radio-quiet AGN shows MAD_s with $a < 0.1$. For Tchekhovskoy (2012) [50] retrograde BH_s appear to have less powerful jets while thicker disks show more powerful jets.

The two-fluid jet model assumes that: 1) the outflow consists of an electron-proton plasma (the jet), moving at mildly relativistic speed, 2) an electron-positron plasma (the beam) is moving at highly relativistic speed, and 3) the magnetic field lines are parallel to the flow in the beam and the mixing layer, and are toroidal in the jet. To confirm and investigate this jet structure Liu (2012) [28] model-fit the MOJAVE blazar core sample which includes blazars with more than 10 years of VLBA monitoring, and more than 15 observed epochs with a good time distribution. This sample consists of 104 sources, 77 of which are quasars, 27 BL Lacs, in which 82 are Fermi-LAT detected, and 22 non-detected sources. Of these, nine are also TeV sources. The model-fit result of the cores of 104 blazars from the MOJAVE monitoring data, for Liu (2012) suggests that Fermi LAT-detected blazars have wider position angle changes of the inner-jet than LAT non-detected blazars, and are preferentially associated with higher variable blazars. A two-zone jet model can explain the correlations in the model-fitted parameters. The Fermi GeV

gamma-ray detection rate show equally similar fraction for sources dominated by the innermost jet (zone-1) and sources dominated by the outer jet (zone-2). But importantly, TeV gamma-ray sources are associated mostly with blazars dominated by the outer part of inner-jet (zone-2).
In conclusion, a relevant problem in AGN is where the high-energy emission is located: close to the Black Hole within the BLR or further down in the parsec-scale jet? Correlations can be used to locate the unresolved gamma-ray emission site. We can have a flux-flux correlation (amplitude domain) or a light curve cross-correlation (time domain). For Hovatta (2012) [23] using simultaneous data, an intrinsic radio/gamma-ray flux density correlation is confirmed. FSRQ$_s$ and BL Lacs show a different behavior (a possible selection effect?). Using archival non-contemporaneous data to increase the statistics, the correlation persists (it is even stronger for BL Lacs because of more sources). More difficult is to tell if individual events are correlated and what are the time delays. Light curve correlations are difficult to establish in single sources. Opacity effects are important in the radio bands, moreover, we could still have too short time series. Stacked correlations show statistically significant time delays with increasing delays for longer wavelengths. Good multiwavelength coverage is really necessary to address this issue.

3.2 Recent studies

3.2.1 The radio/gamma-ray connection in Fermi-blazars

Ghirlanda et al. (2010) studied the correlation between the gamma-ray flux, averaged over the first 11 months of Fermi survey and integrated above 100 MeV, and the radio flux density (F_r at 20 GHz) of Fermi sources associated with a radio counterpart in the AT20G survey. Considering the blazars detected in both bands, the correlation is highly significant, similar for BL Lac and FSRQ sources. However, only a small fraction gamma$_r$ (1/15) of the AT20G radio sources with flat radio spectrum, are detected by Fermi. To understand if this correlation is real, they examine the selection effects introduced by the flux limits of both the radio and gamma-ray surveys, and the importance of variability of the gamma-ray flux. After accounting for these effects, they found that the radio/gamma-ray flux correlation is real, but its slope is steeper than the observed one.
They showed that a strong correlation exists between the radio luminosity and the gamma-ray one and that, considering FSRQs and BL Lac objects, it is linear. They also verified, through partial correlation analysis, that this correlation is not due to the common dependence of the luminosities on redshift for FSRQs (null hypothesis probability of the partial correlation, removing the redshift dependence), while only a marginal claim can be made for BL Lacs alone.
The observed F_γ-F_r correlation and the fraction of radio sources detected by Fermi is reproduced assuming a long term gamma-ray flux variability following a log-normal probability distribution. Such a variability is compatible, even if not necessarily equal, with what observed when comparing, for the sources in common, the EGRET and the Fermi gamma-ray fluxes (even if the Fermi fluxes are averaged over 1 year). Another indication of variability is the non detection of 12 out of 66 EGRET blazars by Fermi, despite its higher sensitivity. They also study the strong linear correlation between the gamma-ray and the radio luminosity of the 144 AT20G-Fermi associations with known redshift and show, through partial correlation analysis, that it is statistically robust. Two possible implications of these correlations are discussed: the contribution of blazars to the extragalactic ray background and the prediction of blazars that might undergo extremely high states of gamma-ray emission in the next years.

3.2.2 The radio/gamma-ray connection in active galactic nuclei in the era of the Fermi Large Area Telescope.

Ackemann et al. (2011) [2] present a detailed statistical analysis of the correlation between radio and gamma-ray emission of the active galactic nuclei (AGNs) detected by Fermi during its first year of operation, with the largest data sets ever used for this purpose. They use both archival interferometric 8.4 GHz data (from the Very Large Array and ATCA, for the full sample of 599 sources) and concurrent single-dish 15 GHz measurements from the Owens Valley Radio Observatory (OVRO, for a sub sample of 199 objects). Their unprecedentedly large sample permits us to assess with high accuracy the statistical significance of the correlation, using a surrogate data method designed to simultaneously account for common-distance bias and the effect of a limited dynamical range in the observed quantities. They find that the statistical significance of a positive correlation between the centimeter radio and the broadband (E $>$ 100 MeV) gamma-ray energy flux is very high for the whole AGN sample, with a probability of $< 10^7$ for the correlation appearing by chance. Using the OVRO data, they find that concurrent data improve the significance of the correlation from 1.6×10^{-6} to 9.0×10^{-8} . Their large sample size allows to study the dependence of correlation strength and significance on specific source types and gamma-ray energy band. They find that the correlation is very significant (chance probability $< 10^7$) for both flat spectrum radio quasars and BL Lac objects separately.
However, the distribution of sources along the correlation has appreciable scatter (which can be typically an order of magnitude). Therefore, they strongly caution that any use of this intrinsic connection between radio and gamma-ray emission in statistical descriptions of the gamma-ray population, such as to obtain gamma-ray luminosity functions from radio luminosity functions, should be done with care and always accounting for the scatter involved. When comparing archival with concurrent data they find that the moderate significance of a correlation derived from the archival radiogamma-ray sample increases appreciably when concurrent data are used.
A dependence of the correlation strength on the considered gamma-ray energy band is also present, but additional data will be necessary to constrain its significance.

3.2.3 The Connection between Radio and gamma-Ray Emission in Fermi/LAT Blazars

Xu-Liang Fan et al. (2012) [53] collect the 2LAC and MOJAVE quasi-simultaneous data to investigate the radio-gamma connection of blazars. The cross sample contains 166 sources. The statistic analysis based on this sample confirms positive correlations between these two bands, but the correlations become weaker as the gamma-ray energy increases. The statistic results between various parameters show negative correlations of gamma-ray photon spectral index with gamma-ray loudness for both FSRQs and BL Lacertae objects, positive correlations of gamma-ray variability index with the gamma-ray loudness for FSRQs, a negative correlation of the gamma-ray variability index with the gamma-ray photon spectral index for FSRQs, and negative correlations of gamma-ray photon spectral index with gamma-ray luminosity for FSRQs. These results suggest that the gamma-ray variability may be due to changes inside the gamma-ray emission region like the injected power, rather than changes in the photon density of the external radiation fields, and the variability amplitude tends to be larger as the gamma-rays are closer to the high energy peak of spectral energy distribution. No correlation of variability index found for BL Lacertae objects implies that variability behavior may differ below and above the peak energy.
In summary, the radio and gamma-ray emission are in good connection in Fermi/LAT blazars, but these correlations become worse as the gamma-ray energy increases. Moreover, the flux correlations would be affected strongly by the selection effects. The gamma-ray variability index is correlated with other parameters for FSRQs. These correlations suggest that the gamma-ray variability may be due to changes inside the gamma-ray emission region like the injected power, rather than changes in the photon density of the external radiation field, and the variability amplitude tends to be larger as the gamma-rays are closer to the high energy peak of SED. The different variability behaviors below and above the peak energy may cause the different trends of BL Lacs and FSRQs. The negative correlations of the gamma-ray luminosity with gamma-ray photon spectral index suggest that the gamma-ray luminosity in Fermi range can not be used simply to investigate the blazar sequence instead of the the peak luminosity or the total luminosity, at least for FSRQs. However, their results are also limited by the source number of their sample, especially for BL Lacs. These results will be tested with larger samples.

3.2.4 On the connection between radio and gamma-rays. Variability and polarization properties in relativistic jets

Orienti et al. (2013) [37] showed that from the comparison of the radio and gamma-ray light curves of gamma-ray flaring objects, there is evidence that some flares, either in radio or in gamma rays, have not an obvious connection at the other extreme of the electromagnetic spectrum, like in the case of the Narrow-Line Seyfert 1 SBS 0846+513. An intriguing aspect pointed out by high resolution radio observations is the change of the polarization properties close in time with some high energy flares. In particular, in PKS 1510089 and 3C 454.3 a rotation of almost 90 degrees has been observed after strong gamma-ray flares. The swing of the polarization angle may be related either to the propagation of a shock along the jet that orders the magnetic field, or a change of the opacity regime.

3.2.5 Connecting radio variability to the characteristics of gamma-ray blazars

Richards et al. (2013) [41] present results from four years of twice-weekly 15 GHz radio monitoring of about 1500 blazars with the Owens Valley Radio Observatory 40 m telescope. Using the intrinsic modulation index to measure variability amplitude, theye found that, with $> 6\sigma$ significance, the radio variability of radio-selected gamma-ray-loud blazars is stronger than that of gamma-ray-quiet blazars. Their extended data set also includes at least 21 months of data for all AGN with clean associations in the Fermi Large Area Telescope First AGN catalogue, 1LAC. With these additional data they examine the radio variability properties of a gamma-ray-selected blazar sample. Within this sample, they found no evidence for a connection between radio variability amplitude and optical classification. In contrast, for their radio-selected sample they found that the BL Lac object subpopulation is more variable than the flat spectrum radio quasar (FSRQ) subpopulation. Radio variability is found to correlate with the synchrotron peak frequency, with low and intermediate-synchrotron-peaked blazars varying less than high-synchrotron-peaked ones. They found evidence for a significant negative correlation between redshift and radio variability among bright FSRQs.

3.2.6 The connection between the 15 GHz radio and gamma-ray emission in blazars

Max-Moerbeck et al. (2014) [31] since mid-2007 have carried out a dedicated long-term monitoring programme at 15 GHz using the Owens Valley Radio Observatory 40 meter telescope (OVRO 40m). One of the main goals of this programme is to study the relation between the radio and gamma-ray emission in blazars and to use it as a tool to locate the site of high energy emission. Using this large sample of objects they are able to characterize the radio variability, and study the significance of correlations between the radio and gamma-ray bands. They found that the radio variability of many sources can be described using a simple power law power spectral density, and that when taking into account the red-noise characteristics of the light curves, cases with significant correlation are rare. They note that while significant correlations are found in few individual objects, radio variations are most often delayed with respect to the gamma-ray variations. This suggests that the gamma-ray emission originates upstream of the radio emission. Because strong flares in most known gamma-ray-loud blazars are infrequent, longer light curves are required to settle the issue of the strength of radio-gamma cross-correlations and establish confidently possible delays between the two. For this reason continuous multiwavelength monitoring over a longer time period is essential for statistical tests of jet emission models.

3.2.7 Radio and gamma-ray connection in relativistic jets

Orienti et al. (2014) [36] showed that recent high resolution radio observations of flaring objects locate the high-energy emitting region downstream the jet at parsec scale distance from the central engine, posing questions on the nature of the seed photons upscattered to gamma-rays. Furthermore, monitoring campaigns of the most active blazars indicate that not all the high energy flares have the same characteristics in the various energy bands, even from the same source, making the interpretation of the mechanism responsible for the high-energy emission not trivial. Although the variability of the most luminous blazars is well explained by the shock-in-jet scenario, the sub-class of TeV emitting objects suggests a more complex emission model with velocity gradients in a structured jet. Orienti et al. presents results obtained by recent multiwavelength campaigns of blazars aimed at studying the radio and gamma-ray connection and the physical mechanisms at the

basis of the emission in these low and high energy bands.

3.2.8 The connection between radio and high energy emission in black hole powered systems in the SKA era

Giroletti et al. (2015) [16] showed that strong evidence exists for a highly significant correlation between the radio flux density and E > 100 MeV gamma-ray energy flux in blazars revealed by the Fermi Gamma-ray Space Telescope. However, there are central issues that need to be clarified in this field: what are the counterparts of the about 30% of gamma-ray sources that are as yet unidentified? Are they just blazars in disguise or they are something more exotic, possibly associated with dark matter? How would they fit in the radio-gamma ray connection studied so far? With their superb sensitivity, SKA1-MID and SKA1-SUR will help to resolve all of these questions. Even more, while the radio-MeV/GeV connection has been firmly established, a radio-VHE (Very High Energy, E > 0.1 TeV) connection has been entirely elusive so far. The advent of CTA (Cherenkov Telescope Array) in the next few years and the expected CTA-SKA1 synergy will offer the chance to explore this connection, even more intriguing as it involves the opposite ends of the electromagnetic spectrum and the acceleration of particles up to the highest energies. We are already preparing to address these questions by exploiting data from the various SKA pathfinders and precursors. They have obtained 18 cm European VLBI Network observations of E > 10 GeV sources, with a detection rate of 83% (and higher than 50% for the unidentified sources). Moreover, they are cross correlating the Fermi catalogs with the Murchinson Widefield Array commissioning survey: when faint gamma-ray sources are considered, pure positional coincidence is not significant enough for selecting counterparts and it is necessary an additional physical criterion to pinpoint the right object. It can be radio spectral index, variability, polarization, or compactness, needing high angular resolution in SKA1-MID; timing studies can also reveal pulsars, which are often found from dedicated searches of unidentified gamma-ray sources. SKA will be the ideal instrument for investigating these characteristics in conjunction with CTA. A proper classification of the unidentified gamma- ray sources and the study of the radio-gamma ray connection will be essential to constrain the processes at work in the vicinity of super massive black holes.

3.2.9 My study

Data and results
The gamma-ray sources in this paper are a subset of those in the second Fermi-LAT Catalog (2FGL). The 2FGL is a catalog of high-energy gamma-ray sources detected by the LAT during 24-months of observations from August 2008 (Nolan et al., 2012) [34] A large amount of blazars in the gamma-rays have been detected by the LAT on board the Fermi. I have selected 174 blazars from the 2FGL, of which 132 quasars and 7 BLLac, with the predominance of sources in the Southern Emisphere, associated to radio sources with $F_{5GHz} < 6$ Jy, extracted from the PKS Catalog Cat90.
After a first analysis I have selected the sources with $F_{5GHz} < 2$ Jy in number of 103, for which I report the plots $F_{radio} - F_{gamma}$, obtained in two ways: first considering only the gamma-ray fluxes of the sources identified in the Fermi-LAT box of the camera (first column in the table), and then adding to these ones the fluxes of unknown sources present in the Fermi-LAT box (second column in the table).
The red squares represent the fluxes of unknown sources present in the Fermi-LAT box and the green triangles represent these ones added to the fluxes of the identified sources in the Fermi-LAT box.
Later I have selected the radio sources observed in more recently epoch, in number of 51 objects, extracted from the Australia Telescope 20 GHz (AT20G) Survey (2008), for which I also report the plots $F_{radio} - F_{gamma}$.

0,16	10,8	1,1282	11,9282
0,17	13,104	1,9114	15,0154
0,19	52,862	6,2012	59,0632
0,19	4,9112	0,3859	5,2971
0,19	6,4601	1,1376	7,5977
0,2	7,2525	1,6879	8,9404
0,2	4,9032	0,8044	5,7076
0,22	30,807	3,7983	34,6053
0,22	8,0208	1,7164	9,7372
0,23	1,6718	0,3679	2,0397
0,25	22,383	1,8703	24,2533
0,27	3,859	0,6097	4,4687
0,27	10,366	1,9624	12,3284
0,28	4,973	1,1886	6,1616
0,29	0,89558	0,1624	1,05798
0,3	24,684	3,0123	27,6963
0,31	7,7498	1,47	9,2198
0,31	58,713	9,9567	68,6697
0,31	42,81	1,3163	44,1263
0,33	2,9969	0,707	3,7039
0,33	65,913	6,5464	72,4594
0,34	4,6637	1,1268	5,7905
0,35	45,941	3,9456	49,8866
0,35	5,3396	0,8789	6,2185
0,36	7,2847	0,9402	8,2249
0,36	4,8136	1,1572	5,9708
0,37	24,15	5,3693	29,5193
0,38	23,008	3,6088	26,6168
0,38	1,0007	0,2503	1,251
0,39	8,9853	1,241	10,2263
0,39	50,492	1,9539	52,4459
0,39	8,2689	1,4656	9,7345
0,4	55,626	3,9452	59,5712
0,43	8,2686	1,8559	10,1245

0,43	6,2563	1,3593	7,6156
0,43	2,8846	0,4721	3,3567
0,43	19,197	1,9217	21,1187
0,44	33,331	1,9497	35,2807
0,44	15,501	3,4685	18,9695
0,45	24,117	1,3588	25,4758
0,45	1,4484	0,3216	1,77
0,46	25,456	2,4925	27,9485
0,48	11,328	1,2396	12,5676
0,53	33,759	6,0494	39,8084
0,54	17,528	1,3665	18,8945
0,54	0,09	0,03	0,12
0,55	48,707	4,7876	53,4946
0,56	6,5374	0,8718	7,4092
0,56	18,02	1,7174	19,7374
0,58	46,093	6,4243	52,5173
0,62	0,8	0,2	1
0,63	8,324	1,2003	9,5243
0,63	2,4819	0,4332	2,9151
0,64	11,407	2,6423	14,0493
0,65	47,729	7,6454	55,3744
0,67	15,937	1,81	17,747
0,69	6,9848	1,4632	8,448
0,7	22,137	2,4887	24,6257
0,7	46,192	6,9556	53,1476

Figure 16: Table 3.1

0,74	2,9608	0,6138	3,5746
0,75	35,186	2,6764	37,8624
0,76	2,2149	0,481	2,6959
0,78	7,2274	1,6706	8,898
0,78	24,165	2,9841	27,1491
0,79	11,639	2,4242	14,0632
0,79	35,889	3,1398	39,0288
0,8	2,3787	0,3719	2,7506
0,82	9,6401	1,3648	11,0049
0,84	2,7653	0,4071	3,1724
0,87	42,93	5,6575	48,5875
0,89	33,243	2,5015	35,7445
0,94	15,835	2,6751	18,5101
0,94	1,061	0,2077	1,2687
0,94	5,1041	0,4655	5,5696
0,96	10,712	1,5983	12,3103
0,98	15,957	3,0413	18,9983
1	46,687	3,695	50,382
1,02	30,239	3,8466	34,0856
1,03	11,349	2,4955	13,8445
1,03	4,6787	0,8681	5,5468
1,04	15,316	2,059	17,375
1,06	58,651	3,9205	62,5715
1,17	78,335	5,3058	83,6408
1,18	28,324	1,4295	29,7535
1,19	8,5959	0,566	9,1619
1,22	46,609	2,3684	48,9774

1,29	30,995	3,6107	34,6057
1,31	15,106	1,6511	16,7571
1,32	45,363	4,1403	49,5033
1,32	75,121	6,589	81,71
1,32	42,16	3,1522	45,3122
1,44	62,58	6,9364	69,5164
1,47	44,816	4,1788	48,9948
1,6	33,597	2,9195	36,5165
1,65	51,937	4,7621	56,6991
1,86	48,719	4,3778	53,0968
1,88	98,206	7,0398	105,2458
1,92	67,584	3,3531	70,9371
2,05	55,314	2,4287	57,7427

Figure 17: Table 3.1

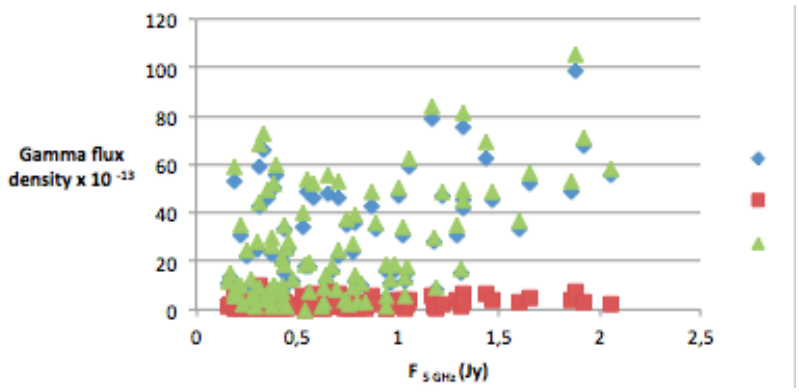

Figure 18: 5 GHz radio flux versus gamma-ray photon flux.

The red squares represent the fluxes of unknown sources present in the Fermi-LAT box and the green triangles represent these ones added to the fluxes of the identified sources in the Fermi-LAT box.
I have also made a partial processing of the data in the new third Fermi-LAT catalog (3FGL) associated to radio sources with $F_{5GHz} < 6$ Jy, extracted from the PKS Catalog Cat90. After a first analysis I have selected the sources with $F_{5GHz} < 3$ Jy (third column in the table 3.3) in number of 114, for which I report the plots $F_{radio} - F_{gamma}$, obtained in this way: considering only the gamma-ray fluxes of the sources identified in the Fermi-LAT box of the camera (second column in the table 3.3).

Discussion

In apparent contrast with the studies published so far the linearity relation in more simultaneous data appear more uncertain (less well defined) compared to the correlation with less simultaneous data. The linear relationship appears more certain (better defined) for the radio sources of the third catalog (3FGL) with 5 GHz radio flux greater than 1 Jy.
The linearity relation also appears more uncertain if we consider only the gamma-ray fluxes of the sources identified in the boxes, whereas it appears more well defined by adding the gamma-ray flux of unknown source revealed in the boxes. This trend appears evident in the correlation both with less simultaneous data and more simultaneous data. A well defined identification of the sources in the Fermi-LAT boxes can be interesting to understand if they can be associated to the already identified sources, as have also been speculated in Giroletti et al., 2015.

0,27	52,862	6,2012	59,0632
0,45	46,192	6,9556	53,1476
0,56	15,106	1,6511	16,7571
0,58	24,684	3,0123	27,6963
0,65	33,331	1,9497	35,2807
0,66	5,7423	0,9621	6,7044
0,7	47,729	7,6454	55,3744
0,71	66,774	7,8552	74,6292
0,9	48,707	4,7876	53,4946
0,95	46,609	2,3684	48,9774
0,98	35,186	2,6714	37,8574
1,04	28,324	1,4295	29,7535
1,07	35,889	3,1398	39,0288
1,17	42,16	3,1522	45,3122
1,21	42,93	5,6575	48,5875
1,23	75,121	6,589	81,71
1,25	15,835	2,6751	18,5101
1,35	11,639	2,4242	14,0632
1,38	46,047	3,0243	49,0713
1,43	58,651	3,9205	62,5715
1,45	10,712	1,5983	12,3103
1,54	45,363	4,1403	49,5033
1,56	51,937	4,7621	56,6991
1,65	62,58	6,9364	69,5164
1,99	10,209	2,3754	12,5844
2	2,9104	0,5744	3,4848
2,01	3,295	0,6547	3,9497
2,35	72,355	5,3058	77,6608
2,37	44,816	4,1788	48,9948
2,49	25,943	2,6048	28,5478

Figure 19: Table 3.2

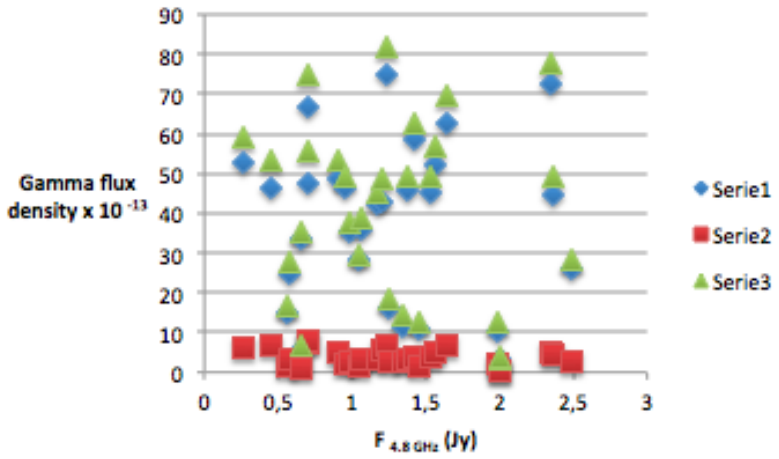

Figure 20: 4.8 GHz radio flux versus gamma-ray photon flux.

4 Studies of radio galaxies with CTA

4.1 Introduction

"In the field of observation, chance only favours the prepared mind." - Louis Pasteur (1854).

It is a truism that major advances in astronomy have usually followed the introduction of a new tool. In 1610 Galileos improved "spyglass" dramatically revealed the four moons of Jupiter, illustrating that not all celestial bodies orbit the Earth, contrary to the then prevailing view. In the report of this momentous discovery, Galileo wrote: "I propose great things for inspection and contemplation, by every explorer of Nature. Great, I say, because of the excellence of the things themselves, because of their newness unheard of through the ages, and also because of the instrument with the benefit of which they make themselves manifest to our sight." His advice has been followed with great success by subsequent researchers, leading e.g. to the serendipitous discovery of the cosmic microwave background in 1965 using a horn antenna designed to relay telephone calls via satellite, and of pulsars in 1967 using a radio telescope designed to study rapid time variations in the signal from quasars. The first X-ray detector carried aboard a sounding rocket in 1962 saw a powerful source in the sky that turned out to be a neutron star binary. Subsequent observations of X-ray sources led to the discovery of stellar black

1	0,16	1,12
2	0,17	0,69
3	0,19	1,59
4	0,19	3,23
5	0,2	0,97
6	0,2	0,68
7	0,22	0,92
8	0,22	0,54
9	0,25	2,13
10	0,27	1,18
11	0,27	0,54
12	0,27	0,83
13	0,28	0,29
14	0,31	0,41
15	0,31	0,69
16	0,33	0,63
17	0,33	1,13
18	0,34	0,29
19	0,35	2,56
20	0,36	0,24
21	0,36	1,22
22	0,37	1,43
23	0,38	0,51
24	0,38	0,68
25	0,39	0,54
26	0,4	1,84
27	0,43	0,38
28	0,43	3,05
29	0,43	0,91
30	0,44	2,79
31	0,45	3,11
32	0,45	0,44
33	0,48	1,42
34	0,49	1,28
35	0,51	3
36	0,52	1,28
37	0,53	0,74
38	0,53	2,76
39	0,56	0,86
40	0,56	2,04

Figure 21: Table 3.3

41	0,57	2,22
42	0,58	2,78
43	0,59	1,83
44	0,59	4,53
45	0,59	1,26
46	0,63	1,07
47	0,63	0,58
48	0,64	1,66
49	0,65	0,55
50	0,67	1,4
51	0,7	0,57
52	0,7	2,78
53	0,7	3,39
54	0,74	0,33
55	0,75	3,36
56	0,76	0,59
57	0,77	1,76
58	0,78	0,43
59	0,78	0,77
60	0,79	0,32
61	0,79	1,53
62	0,8	1,1
63	0,82	2,75
64	0,82	0,4
65	0,84	0,95
66	0,87	0,75
67	0,89	1,86
68	0,9	1,36
69	0,94	0,62
70	0,94	0,53
71	0,96	0,38
72	0,97	1,92
73	0,98	0,92
74	0,98	0,83
75	0,99	0,79
76	1,01	2,46
77	1,02	0,49
78	1,03	0,24
79	1,04	1,33
80	1,06	1,65

Figure 22: Table 3.3

81	1,06	4,04
82	1,15	0,65
83	1,17	1,83
84	1,18	3,69
85	1,19	3,55
86	1,22	4,93
87	1,31	1,12
88	1,32	1,5
89	1,32	2,3
90	1,32	0,79
91	1,38	0,86
92	1,4	3,49
93	1,44	0,88
94	1,47	0,87
95	1,58	1,06
96	1,6	1,87
97	1,65	1,02
98	1,73	4,33
99	1,84	1,46
100	1,85	2,73
101	1,88	1,2
102	1,92	3,62
103	2	3
104	2,04	3
105	2,05	5,48
106	2,28	2,92
107	2,34	1,76
108	2,45	6,34
109	2,46	3,72
110	2,48	0,44
111	2,5	1,43
112	2,6	4,6
113	2,67	1,12
114	2,75	3,58

Figure 23: Table 3.3

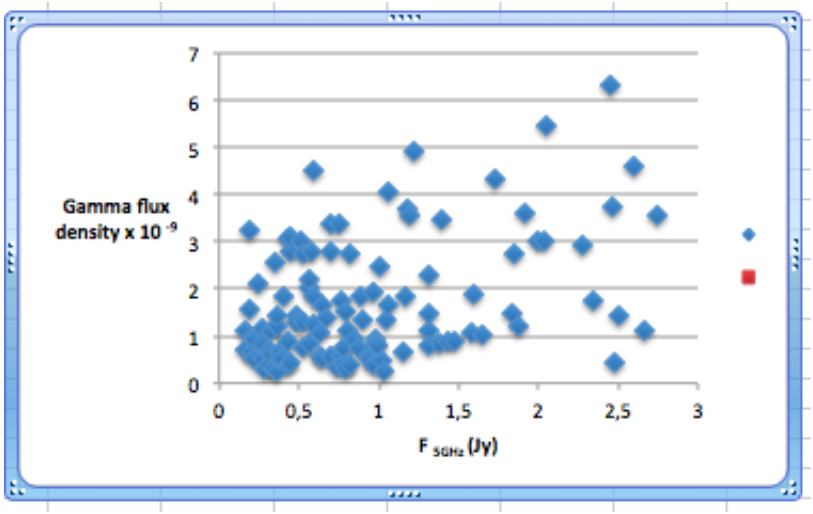

Figure 24: 5 GHz radio flux versus gamma-ray photon flux.

holes. In his influential book "Cosmic Discovery" (1981), the astronomer Martin Harwit [21] provided many such examples and noted in addition that the innovators are frequently not professional astronomers themselves, but rather physicists or engineers. (Harwit also argued against construction of major international facilities like the Hubble Space Telescope on the grounds that it would be unlikely to discover anything really new; however subsequent major discoveries, e.g. dark energy, exoplanets etc., have shown this fear to be quite unfounded.

Another window on the sky that opened up just over two decades ago is high-energy gamma-ray astronomy using ground-based Imaging Atmospheric Cherenkov Telescopes. Following pioneering attempts in the 1960s led by Chudakov and Zatsepin in the USSR and Jelley and Porter in the UK, the field began effectively in 1989 with the first robust detection of the Crab Nebula in TeV gamma rays using the 10-m diameter IACT at the Whipple Observatory. This activity has grown rapidly to become one of the most productive sub-fields of astrophysics today, with modest investments leading to many exciting discoveries with experiments like H.E.S.S., MAGIC and VERITAS. Over 100 sources are now known (http:// tevcat.uchicago.edu), many of them unanticipated and many more yet unidentified. Among the identified sources, which have been subjected to morphological, spectroscopic and temporal studies are active galactic nuclei (BL Lac), starburst galaxies,

pulsar wind nebulae, shell-type supernova remnants, Wolf-Rayet stars, giant molecular clouds, X-ray binaries and the Galactic Centre. IACTs have also provided sensitive probes of dark matter annihilation in the Galaxy and in the satellite dwarf spheroidal galaxies, and of possible high-energy Lorentz invariance violation due to quantum gravity effects. Another application has been as a probe of the extragalactic background light, which would attenuate TeV radiation from very distant sources, as well as measurement of high-energy cosmic-ray electrons and nuclei. Overviews of this remarkable progress have been given in several excellent reviews (e.g.ARNPS 47 (2009). The next logical step in this enterprise is the Cherenkov Telescope Array (CTA). This will provide increased sensitivity, wider energy coverage, better angular resolution, superior energy resolution, and a wider field of view than existing instruments. Over 1000 scientists and engineers in 170 institutions in 27 countries are engaged presently in the prototyping of the concepts formulated in a Design Study, which was conducted during 2008-11 (CTA Consortium, Experimental Astronomy 32 (2011) and construction is scheduled to occur during 2018. There will be two sites, one in the Southern hemisphere which will focus on galactic sources, and one in the Northern hemisphere aimed mainly at extragalactic studies. For the first time in this astronomical field, CTA will be operated as an open observatory.

"The only true voyage of discovery, the only fountain of Eternal Youth, would be not to visit strange lands but to possess other eyes, to behold the universe through the eyes of another, of a hundred others, to behold the hundred universes that each of them beholds, that each of them is." (M. Proust).

In spite of their small number, the non-blazar gamma-ray emitters are extremely appealing, as they offer a powerful physical tool in approaching the high energy phenomena. ($MAGN_s$ are Radio Galaxies and Steep Spectrum Radio Quasars, i.e. Radio Loud objects with steep radio spectra and/or showing possibly symmetrical extension in radio maps.)

We argue that CTA will enable substantial progress on gamma-ray population studies by deepening existing surveys both through increased flux sensitivity and by improving the chances of detecting a larger number of radio galaxies.

The high energy jet emission discovered in NLSY1s is questioning the paradigm according to which radio-loud AGNs are only hosted in elliptical galaxies. The detection of gamma-ray photons in $MAGN_s$ is invaluable in revealing the jet structure complexity.

The LAT detection of several objects in the GeV sky exploration has succes-

sively confirmed MAGN$_s$ (Misaligned AGN) to be a new class of gamma-ray emitters. Among MAGN$_s$, only three source, i.e. 3C111, Centaurus A and NGC6251, have been proposed as candidates by the previous γ-ray telescope EGRET. The other ones represent a new discovery. Most of the sources of the 15month-MAGN sample are faint and have steep power law spectra. This is in general agreement with the AGN Unified Models that assume MAGNs to be a de-boosted version of blazars. Because of their faintness, variability studies are not conclusive. Only in one case, NGC1275, flux and spectral changes could be statistically ascertained on time scale of months. As a consequence, establishing where the gamma-rays are produced is a difficult task. The variability of NGC1275 seems to suggest a sub-pc scale ($< 10^{18}$ cm) emission region, but the discovery of gamma-ray emission from the radio lobes of Centaurus A shows that extranuclear extended kpc regions can also be sources of high energy photons.

In this chapther, I review the prospects of CTA to facilitate progress in our understanding of the radio galaxies phenomenon and its related physics including the large-scale impact of the associated jets.

I outline the current status of CTA and discuss the science case for radio galaxies physics with the observatory. Predictions for source detections based on extrapolations of Fermi-LAT spectra are discussed. An overview is given of prospects for the detection of extended emission from radio galaxies.

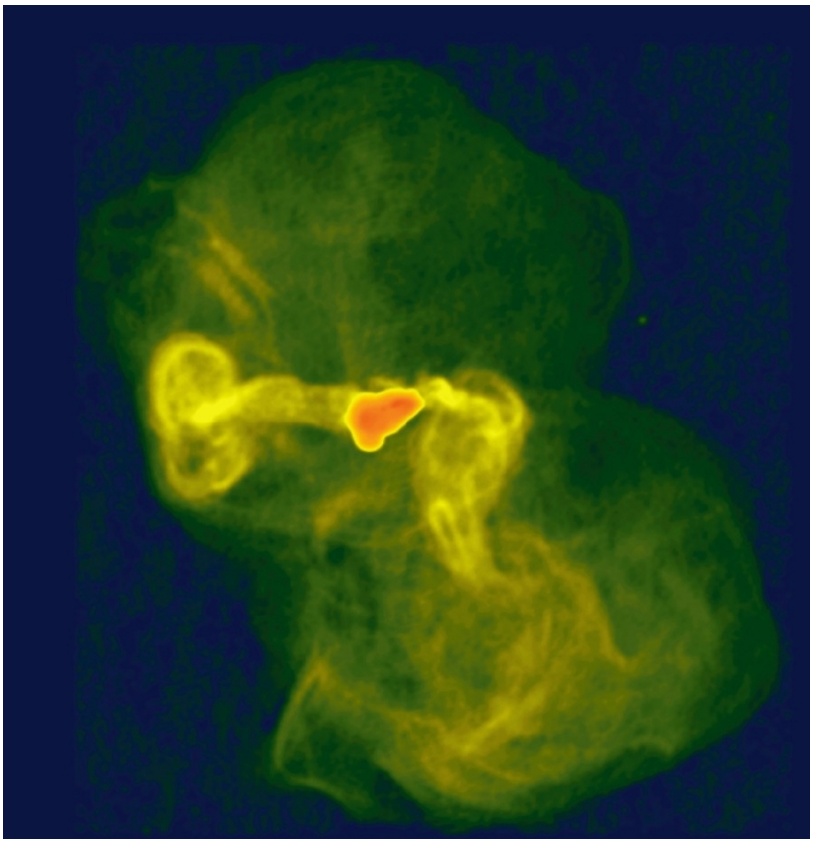

Figure 25: False color image of the radio galaxy M87 (VLA 90 cm.)

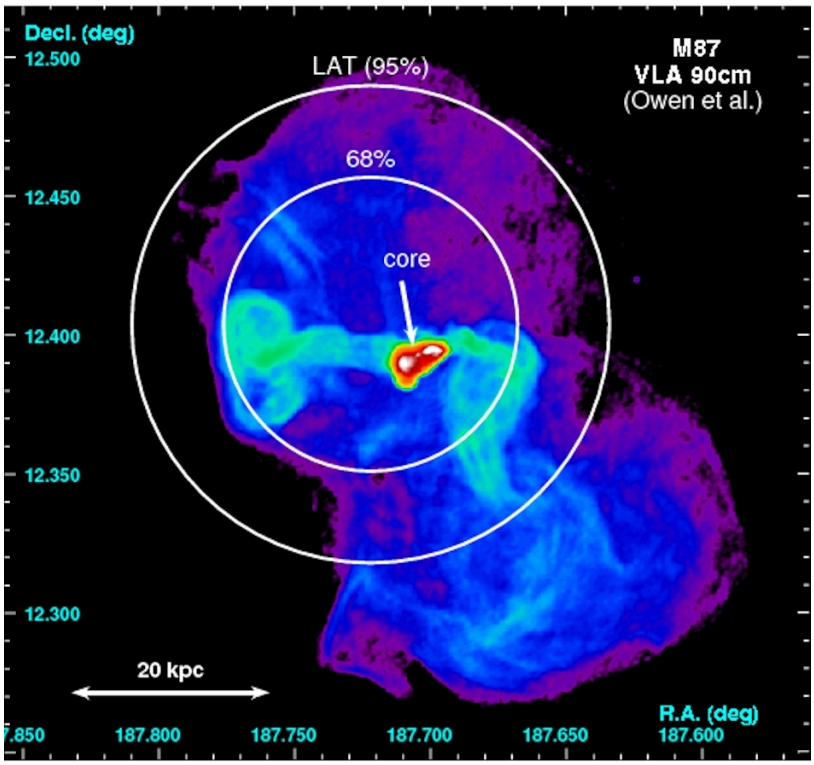

Figure 26: False color image of the radio galaxy M87 superimpressed to Fermi detection.

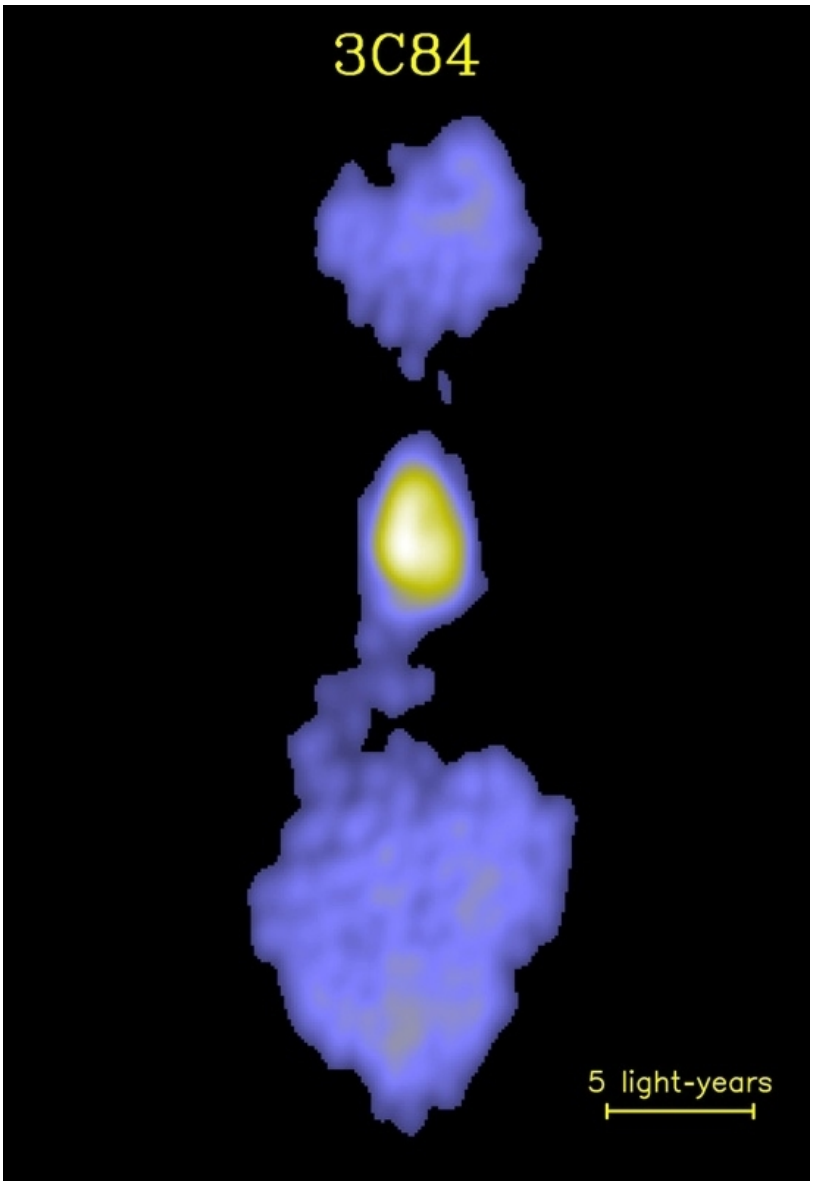

Figure 27: False color image of the radio galaxy NGC 1275.

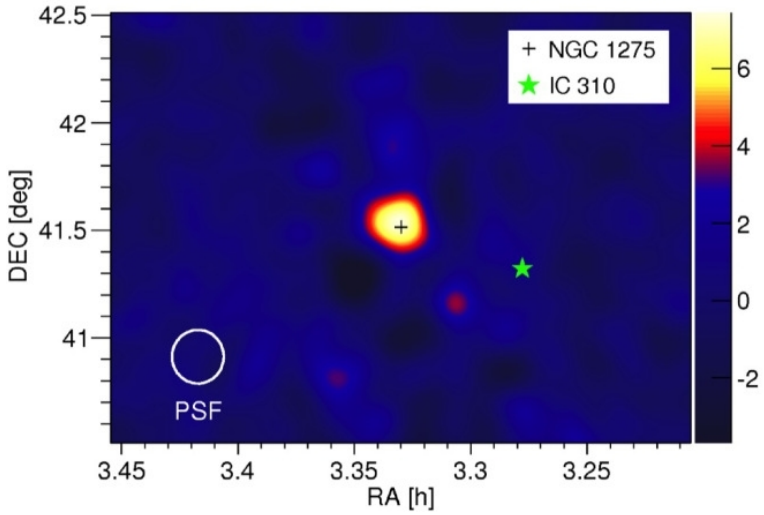

Figure 28: MAGIC false color image of NGC 1275 galaxy (MAGIC Collaboration).

4.2 The Cherenkov Telescope Array

The Cherenkov Telescope Array (CTA) is a new observatory for very high-energy (VHE) gamma-rays. CTA ha ambitions science goals, for which it is necessary to achieve full-sky coverage, to improve the sensitivity by about an order of magnitude, to span about four decades of energy, from a few ten of GeV to above 100 TeV with enhanced angular and energy resolutions over existing VHE gamma-ray observatories.
To meet the physics requirements specified with a high technical performance within a reasonable budget, the CTA concept is based on few general ideas:

- use proven IACT technology;
- increase the array from currently 4-5 telescopes (VERITAS, HESS) to several tens;
- use telescopes of 3 different sizes:
- few (4) large-size telescopes (LST) with=23 m diameter parabolic dishes, optimized for E $<$ 200 GeV region (based on MAGIC), with a 5o FOV, and placed at the center of the array;

- several (20) medium-size telescopes (MST) with=11 m diameter Davies-Cotton dishes, optimized for use in the range 0.1 - 10 TeV, with a 8o FOV, and placed in a central corona of the array surrounding the LST nucleus: these telescopes (based on HESS and VERITAS) will be the core of the array and will also veto the LST triggers in order to reduce the hadronic background;

- many simple-to-build small-size telescopes (SST) with=4 m or 7 m diameter Davies-Cotton or Schwarzschild-Couder dishes, optimized for E > 5 TeV, with a 10o FOV, and scattered over a large area on ground;

- distribute telescopes over a large area (1 - 10 km^2) on the ground;

- provide high automatization liable to remote operation;

- run facility as an open observatory, open to the astrophysics community. In general, a larger number of nuclear LST_s improves the sensitivity at low energies; a larger and more scattered number of LST_s improves the sensitivity at high energies. So for a given budget, the exact number of telescopes of each type, their size and configuration, are being investigated as a function of the arrays overall performance.

Different CTA operation modes will be possible. In the deep-field mode all telescopes will be pointed to the same sky position to maximize sensitivity. In the divergent-pointing different subsets of telescopes could point to different sky positions - to make simultaneous observations of different sources. In the wide-FOV mode, e.g., an all-sky scan can be performed in a time-efficient way at moderate sensitivity.
Two arrays are planned, in the Southern and Northern hemisphere respectively. The Southern array may possibly be the main one, owing to its advantage location in observing the central region of the Milky Way. The Northern array will be mostly devoted to extragalactic observations: in this case, both the small local pairing technical designs, evaluating sites, optimizing the physics return, estimating construction and operation costs, assessing legal/governance/finance schemes, and building telescope prototypes.
CTA was started as a partnership between the HESS and MAGIC collaborations, but several more institutions later joined in. CTA is organized as a consortium that currently comprises >900 scientists and engineers from

>100 institutions in 26 countries world-wide. Since late 2010 the Preparatory Phase of CTA has been taking care of making technical designs, evaluating sites, optimizing the physics return, estimating construction and operation costs, assessing legal/governance/finance schemes, and building telescope prototypes.
The aim is to get first full-array data in 2020. [38]
CTA will answer many of the persisting questions by enabling the detection of more than 1000 sources over the whole sky. CTA builds on the proven tecnique of detecting gamma-ray induced particle cascades in the atmosphere through their Cherenkov radiation, simultaneously imaging each cascade stereoscopically with multiple telescopes, and reconstructing the properties of the primary gamma ray from those images. Trough deployment of about 50-100 telescopes per site at two sites in the southern and the northern hemispheres CTA will achieve full-sky coverage. The improved sensitivity may permit the discovery of completely new and unexpected phenomena.
The properties of the major current and previous air Cherenkov instruments are listed in Table 4.1 [1]

Instrument	Lat (°)	Long (°)	Alt (m)	Telescopes	Area (m²)	Pixels per camera	FoV (°)	Threshold (TeV)	Sensitivity (% Crab) > 1 TeV
H.E.S.S.	−23	16	1800	4	107	960	5	0.1	0.7
H.E.S.S. II	−23	16	1800	1	614	2048	3.2	tbd	tbd
VERITAS	32	−111	1275	4	106	499	3.5	0.07	0.7
MAGIC I+II	29	−18	2225	2	234	1039	3.5	0.03	0.8
CANGAROO-III	−31	137	160	3	57.3	427	4	0.4	15
Whipple	32	−111	2300	1	75	379	2.3	0.3	15
HEGRA	29	18	2200	5	8.5	271	4.3	0.5	5
CAT	42	2	1650	1	17.8	600	4.8	0.25	15

Figure 29: Table 4.1

Besides a wealth of high-energy astrophysics results, CTA will have a large discovery potential in key areas of astronomy, astrophysics and fundamental physics research.
The aim of the CTA is to make is to make significant progress over the existing experiments in every respect of science. In the core science themes there is the Black-Holes and jets. The observations of rather close-by radio galaxies can shed light on the formation of the jet and its connection to the central black-hole properties.
Table 4.2 summarises the performance goals of CTA.

Diff. sensitivity (erg cm^{-2} s^{-1})	at 50 GeV	8×10^{-12}
	at 1 TeV	2×10^{-13}
	at 50 TeV	3×10^{-13} (S) / 10^{-12} (N)
Collection area (m^2)	at 1 TeV	$> 10^4$
	at 10 TeV	$> 10^6$ (S)/$> 5 \times 10^5$ (N)
Angular resolution	at 0.1 TeV	0.1°
	>1 TeV	0.05°
Energy resolution	at 50 GeV	$\leqslant$ 25%
	>1 TeV	$\leqslant$ 10%
Field of view	at 0.1 TeV	5°
	at 1 TeV	8°
	>10 TeV	10°
Sensitivity in FoV	at 1 TeV flat out to	$>$ 2.5°
Source localisation	at 1 TeV	5′ per axis
Repointing time	<0.1 TeV	20 s (goal), 50 s (max)
	0.1–10 TeV	60 s (goal), 90 s (max)

Figure 30: Table 4.2

4.3 Recent studies

4.4 AGN Population Studies for CTA

Inoue [24] discussed the expected number of blazars and highest redshift accessible with future CTA observation based on a recent blazar GLF model. For a blank field sky survey, a wide and shallow search will enable us to carry out an efficient survey. CTA will detect below 50 and below 160 blazars with 1 year and 10 years blank field sky survey, respectively. With CTA, we should be able to find a blazar at z = 1.4 (20 blazars above z = 1). By simply extrapolating the GeV spectrum of the Fermi blazars in the first catalog, CTA is expected to detect a blazar at z = 2.49. This will enable us to study the cosmological evolution of VHE blazars. Although Inoue discussed only blazars in this paper, other classes of AGNs are also expected as potential sources for CTA, such as core emission from radio galaxies, kpc jet emission, low luminous AGN_s. By observing various AGN populations and high redshift sources, CTA will help to unify AGN populations and study the cosmological evolution of the VHE universe.

4.4.1 AGN Physics with the Cherenkov Telescope Array

The detection of radio galaxies in the VHE band raises the question of a possible detection of extended emission from these sources with CTA. Given the typical angular resolution of IACT arrays, this will be a major challenge for even the most nearby sources, Centaurus A (at 3-5 Mpc) and M87 (at about 16 Mpc). Extended emission might in principle be seen from the kpc jets or from the large (100 kpc to Mpc scale) radio lobes of these objects and could teach us about their formation and energetics. Extended emission from the lobes of Centaurus A has been discovered with the Fermi-LAT and seems to be dominated by the Inverse Compton emission of electrons in the lobes upscattering photons from the CMB and EBL. A simple extrapolation to the VHE band of the spectrum measured from the lobes operate by Zech [55] does not predict a detectable signal for CTA. Somewhat more promising might be the emission from the extended jet. A simulation of the VHE emission from this jet leaves the possibility of detecting extended emission beyond 1 arcminute away from the central core with CTA. It should however be emphasized that an angular resolution of this order will only be reached for events with sufficiently high telescope multiplicities, i.e. for gamma-rays of sufficiently high energies, typically not below 10 TeV. Resolving the kpc jet of M87, with an extension of roughly 30 arc seconds, is out of reach for CTA. But even if the jet will not be resolved, good astrometric precision might allow the detection of an offset between the peak of the VHE emission and the nominal source position of the radio core. In the case of M87 for example, the currently projected uncertainty in the absolute pointing might be sufficient to distinguish emission from the central core or from the "knot A" radio structure in the jet. A detection of emission from the radio lobes of M87 with CTA might be possible, if one assumes that 50% of the total flux of the source is distributed over the lobes.

Being able to pinpoint the VHE emission region, even for one or two radio galaxies, would present a milestone for AGN physics at the highest energies. The angular resolution and astrometry of CTA are therefore of real concern for AGN observations. For most of the detected AGN, a direct determination of the VHE emission region is obviously unfeasible, but the excellent sensitivity and energy resolution of CTA will help to characterize the emission region indirectly, through variability studies.

Variability is frequently detected in blazars and radio galaxies and presents our best tool to constrain the size of the emission region of VHE gamma-

rays. Compared to other wavelength bands, this energy range shows the most rapid variability, down to time-scales of a few minutes in the most extreme cases. Given the usual light traveling time arguments, the measurement of the variability time scale Δt_{obs} provides a direct constraint on the size of the emission region R for a given Doppler factor δ.
In the case of the extreme flares from PKS2155-304 in 2006, more than 100 gamma-rays per minute were detected with H.E.S.S., permitting a measurement of time scales down to the minute. Flux doubling times of the order of two to three minutes were measured. A similar flare - admittedly a rare event - when observed with CTA, would yield thousands of gamma-rays per minute, allowing an extension of the search for variability down to a time scale of several seconds. Extremely small emission regions (or extremely high Doppler factors) might be found, further challenging our picture of the emission mechanisms. Alternatively, the detection of a break in the power spectral density would set a lower limit on the variability time scale.
The variability of flaring sources will be studied in detail with data from CTA to characterize the underlying emission processes. A study carried out with H.E.S.S. data from the above mentioned flares found that the detected flux variability corresponds a lognormal process, hinting at an underlying multiplicative mechanism. The implications of this observation are not yet fully understood and our current perception would clearly profit from additional observational evidence.
Equally important as the study of flares will be the search for rapid variability during low states of the sources. It would help answer the question of whether the emission from blazars and radio galaxies is separated into a static, quiescent component to which flaring episodes are added, or whether variability is a general feature at all flux states. This requires a sufficiently high sensitivity to collect good photon statistics at low flux states. With CTA, this should be possible for the most luminous blazars. PKS 2155-304, for example, should provide sufficient statistics for studies at the time scale of a few minutes, even in its low state.
If one wants to not only constrain the size of the emission region, but to pin down the origin of the VHE emission in the source, multiwavelength (MWL) campaigns of blazars and radio galaxies, especially during flares, are today the most promising means at our disposal. Several MWL campaigns on M87, for example, have shown that it is possible to infer the location of the emission region of VHE gamma-rays by studying correlations between VHE and radio flares. This sort of study will certainly benefit greatly from the

improvements in sensitivity and coverage of CTA and from the synergy with new and future radio astronomy facilities, such as e.g. LOFAR and SKA. Furthermore, relations between the flux evolution in the VHE band and in the optical and radio bands, seen recently also in the data from PKS 2155-304, provide important insights into the emission processes and the radiative transfer inside the source.

4.4.2 Active Galactic Nuclei under the scrutiny of CTA

Detection and monitoring of four radio galaxies at TeV energies definitely proved that AGN other than blazars actually radiate at VHE. Indeed, although quite rewarding by itself, detecting only blazars at VHE energies provides biased information about AGN jets, always seen at small viewing angles. Studying AGN with moderate or negligible Doppler boosting with CTA will provide access to a 2D view of AGN jets at VHE and will shed new light on our current understanding of radio-loud AGN. In particular, the performances of CTA should allow a detailed analysis of the relation between VHE and non-thermal radio emission and will contribute to the long-standing question of the origin of radio-loudness in AGN.
The four radiogalaxies detected so far at VHE, namely M 87, Cen A, IC 310, and NGC 1275, have all been tentatively classified in the literature as Fanaroff-Riley type 1 radio sources, each with some "peculiarities". Apart from that, these active galaxies and their nucleus and jets show very different properties which, based on knowledge already gathered at lower energies, do not suggest any specific prominent common features, except being TeV sources. These VHE galaxies form an emerging class of AGN, which should find its place within AGN grand unification. This simple fact illustrates that observing at VHE probes new aspects of AGN not yet explored at any other energies, and offers a fully independent tool of investigation. One possibility would be that the VHE band directly catches the emission from the base of an inner beam or jet when it has a right orientation, independently of any other properties and classification of the radio source at others frequencies.
For Sol et al. [47] this emphasizes the strong interest of studying such types of sources with CTA, but precludes at the moment any convincing prediction of a sample to be detected at VHE in the future. In particular, in the current small sample of VHE radiogalaxies, the average detected TeV fluxes do not seem to be related to the average non-thermal radio and X-ray fluxes of the sources. One common trend is that the four sources are located in rich

environments, and show sign of galaxy interaction or mergers.
Both M 87 and NGC 1275 are dominant cluster galaxies with a very massive central black hole. Cen A is presumably a recent merger, in a group of galaxies, and IC 310 is located in the Perseus cluster where radio jets can interact with the intracluster gas. Other common properties could be to have an intermediate viewing angle (about 20 degrees for M 87, 40 for Cen A, between 20 and 50 for NGC1275 and $\leq$38 for IC 310), weak or moderate Doppler beaming, and no direct alignment between their radio compact VLBI core and their extended radio structures (grossly misaligned by below 70 degrees in M 87 and below 45 degrees in Cen A), possibly enhanced by projection effects and inhomogeneous external medium, or related to specific properties of their central engines. Moreover, the detection of some transient BL Lac-type phenomena has been reported or discussed in the literature for the four radiogalaxies discovered up to now at VHE. Such properties should help to identify promising candidates for further observation with CTA. Among this new class of AGN, M 87, the first non-blazar detected in the VHE range, has been the most studied in the literature. It questions our global understanding of TeV emission scenarios for AGN, and to some extent our general view of AGN classification. Even assuming a high Doppler factor, the TeV variability of M 87 requires very small emitting zones, under causality argument. This raises the critical question of particle acceleration mechanisms in such small regions, and excludes the Virgo cluster, the radio lobes, the host galaxy, the large scale jet and its brightest knot A as dominant TeV emission zones. Three different main emitting zones have been considered for M 87, (i) the peculiar knot HST-1 located at about 65 pc from the nucleus, (ii) the inner VLBI jet, and (iii) the central core itself, namely the accretion disk or the inner black hole magnetosphere.
The coordinated campaign in 2005 found a possible correlation between a VHE flare and an X-ray outburst of HST-1. However, another multi wavelength campaign organized in 2008 concluded that the X-ray light curve of HST-1 obtained by Chandra does not follow the VHE one. Conversely, the radio and X-ray emissions from the core are correlated with the VHE flux. In radio, regular monitoring of M 87 by the VLBA at 43 GHz also allows one to explore the sub-mas scale in order to probe the jet formation and collimation zone at about 100Rs from the black hole, with an outstanding angular resolution of 0.21 mas$\times$0.43 mas (0.5mas=0.04pc=140Rs at the distance of M 87). The VLBA detected a significant rise of the flux of the radio core at the time of the 2008 VHE activity, together with enhanced emission along

the VLBI jet. For Sol et al. these results favour scenarios where most of the VHE emission comes from the inner VLBI jet (multi-zone models inspired from standard blazar scenarios or from the central core (particle acceleration in the black hole magnetosphere. However the situation still remains unclear, and suggests the existence of different types of VHE flares, as discussed in a work reporting on the 2010 large joint monitoring campaign.
Current magnetospheric models for M 87 imply that minimum variability timescale should always be larger than a few Schwarzschild light crossing times Rs/c = (0.2-0.4) days (in the absence of strong Doppler effect) and that the TeV spectra should exhibit a clear break, due to internal $\gamma\gamma$ absorption and maximum energy constraints, well below 50 TeV. Confirming or rejecting such magnetospheric scenarios with "particle acceleration close to the SMBH" by future high-sensitivity observations with CTA would boost our understanding of AGN central engines: in the former case, new jet physics beyond current developments would be demanded, in the latter case, a strong link between jet formation, particle acceleration and disk physics would be established.
In the second radiogalaxy discovered at VHE, the nearby source Cen A, the origin of the dominant VHE signal is even less clear than in M 87, as both the radio core and the kpc jets of Cen A are within error bars of its position on the sky. This results in many possible emitting zones such as the black hole magnetosphere, the base of the jet, the large scale jets and inner lobes, or even a pair halo in the host galaxy. A better accuracy on the absolute astrometry at VHE expected with CTA and obtaining high quality light curves with good temporal coverage should clarify this decisive issue, and at least distinguish between a dominant core emission or a dominant extended component related to the kpc jets. Indeed, very extended diffuse gamma-ray emission has been recently found by Fermi at lower energies. The gamma-ray emission above 100 MeV coming from the giant lobes can be described by EIC models on the cosmic microwave background and the EBL. This emission is quite important, with a total flux slightly higher than the one from the core and a power comparable to the kinetic power required in the jets. For Sol et al. the high sensitivity and improved angular resolution of CTA should allow one to look for and possibly map any extended structure at higher energies, thereby opening a completely new view on VHE particle acceleration, transfer and radiative losses. A simple extrapolation of the Fermi halo to the VHE band shows that its VHE counterpart remains out of reach by CTA, assuming the same spatial extension of about 2 degrees.

However, VHE detection can be expected from regions of enhanced gamma-ray emission in shocks, knots, or hot spots, which could be identified with the angular resolution of CTA. Conversely, for Sol et al. the detection of an extended VHE halo around M 87 would be very challenging but could be possible with CTA, assuming, as seen by Fermi in Cen A, a flux in the lobes of 50% the flux detected in the TeV range during a low state of the source for an extension of 0.2 degrees corresponding to the extension of radio maps. In contrast to the three other VHE radiogalaxies, IC 310 was initially not recognized as having a specifically remarkable non-thermal activity. Its serendipitous discovery at VHE in the field of NGC 1275 emphasized our current poor knowledge on VHE populations. Only recently it appeared in the Fermi catalog and was then identified as a potential TeV source. Two emission zones can be considered, the central engine and the inner jet as commonly described for TeV BL Lacs, or the bow shock created by interaction of the fast moving host galaxy with the intracluster gas. For Sol et al. astrometric and angular resolution capabilities of CTA should distinguish between them. However, the first option appears favored because of the detection of few-dayscale variability. Indeed, IC 310 was already mentioned in the literature as a FR I source which may have a non-thermal activity related to the BL Lac phenomena, but at weaker levels than characterized by the standard definition of BL Lac objects. Moreover recent VLBI data show a blazar-like one-sided core-jet structure at intermediate angle to the line of sight. VHE instruments are therefore possibly on the way to solve the long standing problem of the "missing BL Lac" and to firmly identify the still elusive transition population between beamed BL Lacs and unbeamed FR I galaxies, a difficulty of the standard unification scheme which proposes that BL Lac are FR I radio galaxies seen along their jet axis. Surveys at VHE could have the capability to recognize a population of low luminosity or misdirected BL Lacs, difficult to identify at lower energies, and thus "bridge the gap" between genuine BL Lacs and FRI radio galaxies. For Sol et al. it will be interesting to further investigate such a view in the context of recent blazar classification scenarios.

Generally speaking, nearby radio galaxies offer the opportunity of unique studies of extreme acceleration processes in relativistic jets and in the vicinity of supermassive black holes. Given the proximity of the sources and the larger jet angle to the line of sight compared to BL Lac objects, the outer and inner kpc jet structures are potentially resolvable by CTA, enabling us to look for possible VHE radiation from large scale jets and hot spots besides the central

core and VLBI jet, and to spatially pin down the main site of the emission. With the help of simultaneous multi wavelength observations and temporal correlation studies, different sections of the jet and the core can be probed, down to the smallest pc (milliarcsecond) scale, only accessible to VLBI radio observations or timing analysis. For Sol et al. further studies of variability with CTA will strengthen the limits on the size of the emission region and clarify the correlations with other wavelengths. Long-term monitoring and the search for intra-night variability would be two major goals to constrain the physics and start characterizing this new population of sources. Remembering the basic classification of extra-galactic radio sources, one could consider highly variable VHE radio galaxies as likely core-dominated gamma-ray sources, and poorly variable ones as possibly lobe-dominated gamma-ray sources. This VHE population is still lacking a standard unifying model and deserves further analysis.
Recent and fast developments on VHE radio galaxies show that present VHE instruments start to provide an original view of non-thermal activity from central AGN engines and inner jets, with the capability to directly probe a very specific region, still not fully identified and unreachable by other means, in the close vicinity of SMBH, such as for M 87. The next generation of IACT will explore this still missing link between SMBH (Supermassive BH) magnetospheres and the physics of jets and extended radio sources. One can also anticipate that it could provide decisive constraints on the fundamental question of the total energy budget of some non-thermal sources where the contribution of the extended gamma-ray emission appears quite significant, such as for Cen A.

4.5 My study

Using the probably correlation between the radio brightness and the VHE γ-ray and considering the expected sensitivity of CTA, it was estimated that with this system of telescopes it will be possible to reveal at least 82 radio galaxies, extracted from various radio catalogs to the frequency of 5 GHz. Definitely a considerable increase in ratio to 4 actually observed with HESS and MAGIC. This number, which is therefore of the order of hundreds, is an estimate because both sites that the configurations of the telescopes of the CTA are not yet fully defined.
Table 4.3 shows the 5 GHz fluxes and the estimated gamma-ray fluxes.

From the analysis of the estimate of the distribution of radio galaxies as a function of redshift it was observed that the majority of them is located at distances z between 0.01 and 0.05, so relatively close.
Figure 33 shows the number of the radio galaxies versus the redshift in the Southern Emisphere.
In conclusion, a study apparently circumscribed as that of radio galaxies observed in the future with the CTA, can contribute to a greater understanding of the phenomenon and the validation of the AGN unified schemes for the various classes.

Source	Fr (5 GHz)	F (gamma) x 10^(-12)
B2 0206+35	0,911	4,7
B2 0755+37	1	5,77
B2 001+34	0,528	2,7
B2 0113+40	0,225	1,16
B2 0132+37	0,31	2
B2 0223+35	0,273	1,41
B2 0704+35	0,195	1,01
B2 0727+35	0,247	1,27
B2 0824+35	0,626	3,23
B2 0847+37	0,324	1,67
B2 0857+39	0,201	1,04
B2 0908+37	0,279	1,44
B2 0922+36B	0,234	1,21
B2 0936+36	0,713	3,68
B2 0938+39	0,768	3,96
B2 1014+39A	0,526	2,71
B2 1025+39	0,328	1,69
B2 1101+38	0,714	3,68
B2 1107+37	0,704	3,63
B2 1141+37A	0,384	1,98
B2 1151+38	0,384	1,98
B2 1322+36B	0,458	2,36
B2 1323+37	0,458	2,36
B2 1336+39	0,947	4,89
B2 1529+35	0,504	2,6
B2 1615+35B	0,477	2,46
B2 1632+39	0,392	2,02
B2 1652+39A	1,242	6,41

Figure 31: Table 4.3

2Jy 1136-13		1,9		9,8
2Jy 0945+07		2,64		13,6
2Jy 0915-11		13,8		71
2Jy 0859-25		1,74		8,9
2Jy 0806-10		1,63		8,4
2Jy 0625-53		1,85		9,5
2Jy 0620-52		1,25		6,4
2Jy 0442-28		2,21		11,4
2Jy 0427-53		3,41		17,6
2Jy 0349-27		2,04		10,5
2Jy 0325+02		1,99		10,3
2Jy 0320-37		72		370
2Jy 0305+03		3,65		18,8
2Jy 0255+05		1,98		10,2
2Jy 0131-36		4,08		21
2Jy 0055-01		2,2		11
2Jy 0043-42		2,98		15,4
2Jy 0034-01		1,6		8,2
2Jy 1318-43		1,75		9
2Jy 1322-42		62,8		320
2Jy 1333-33		6,3		32,5
2Jy 1559+02		2,87		14,8
2Jy 1602+01		1,13		5,8
2Jy 1637-77		2,61		13,5
2Jy 1648+05		12,74		65,7
2Jy 1717-00		20,54		105,9
2Jy 1733-56		3,37		17,4
2Jy 1839-48		1,28		6,66
2Jy 1932-46		3,47		17,9
2Jy 1938-15		2,34		12,1
2Jy 1949+02		2,39		12,3
2Jy 1954-55		2,31		11,9
2Jy 2058-28		2		10,3
2Jy 2104-25		4,31		22,2
2Jy 2152-69		12,65		65,3
2Jy 2211-17		2,14		11
2Jy 2221-02		2,28		11,8
2Jy 2250-41		1,27		6,6
2Jy 2314+03		1,33		6,9

Figure 32: Table 4.3 continue ...

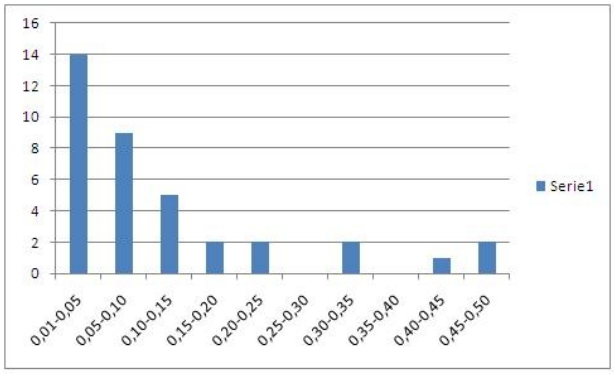

Figure 33: Overview of the plot: number of radio galaxies versus the redshift

5 My study: NGC 326, a peculiar radio galaxy

NGC 326 is a double system composed by two bright elliptical galaxies in a common envelope (Dumbell galaxies) and it is the more bright member of a small group of galaxies (Zwichy 0056.9 + 2636) located at a distance of 141 h-1 Mpc, with a magnitude of 13,9 [6]. NGC 326 has been well studied in the optical band (HST), radio band (VLBA) and in the X-ray band (CHANDRA) but it has not been revealed in gamma-ray band, also as upper limit (it is not in the Fermi/Lat list). NGC 326 is one of the more prominent radio galaxy with Z-shaped morphology and it has been object of several studies to explain its peculiar morphology of the reorientation of the axis of the jet. The jet, the lack of hot spots, and the low radio power (10^{41} erg s^{-1}) indicate a faint FR I radio source today, but the front of the shock, the dimension of the lobe and its morphology, and the GHz emission, indicate a powerful FR II radio source not more than 30 Milions of years ago [22].
The Z-shaped morphology of 3C 326 is modeled by the velocity variation of the jet, combined with an appropriate composition of the precession velocity of the jet [54].
Recent observations of gamma-ray VHE emission from the radio galaxies M 87, Centaurus A, IC 310 and NGC 1275, have defined a new class of gamma-ray sources: the radio galaxies. The radio galaxies are AGN but their jets

shows a large angle with the line of sight and so their emission is less boosted (NGC 326 showed a large angle of orientation (>60 degrees), as in [29]. This different geometry, moreover, permit to study the individual components of the AGN system with more detail. More important: the major part of the more close AGN are radio galaxies. P. Grandi et al (2011) [18] predicted that more than 10% of the FR I radio galaxies of the sample obtained by the combination of the catalogues 3CR, 3CRR, MS4 and 2 Jy have gamma-ray emission. Its detection appear to be favored by the presence of different velocity zone in the jet. The location of the gamma-ray emission in a radio source is still unknown, but the core, the internal jet or more large structures in the jet, can be possible sites.
NGC 326 is situated in a cluster of galaxies. The clusters of galaxies are seat of different kinds of energetic outflows of powered source, type radio galaxies, and they present a large amount of gas with embedded magnetic fields. Therefore it can be interesting targets for the detection of gamma-ray emission, which can be also explained in the hadronic scenario, were the electrons radio emitting are produced in hadronic interactions CR p-p with protons of the intra cluster medium [30]. Moreover to predict gamma-ray emission in the radio galaxies, also hadronic models have been proposed.
By considering that NGC 1275 (the fourth nearby radio galaxy detected by MAGIC) appear to exhibit in the radio band a jet precession which has been interpreted as possible indication of a merger of two galaxies [5], we propose the radio galaxy NGC 326 as a possible candidate for detection with the future CTA, for this reasons:

- Its relative proximity;
- Its morphological similitude with NGC 1275;
- Its historical FR I radio morphology and its core dominance;
- Its more brightness in an Elliptical Dumbell system;
- Its location in a cluster of galaxies, in a more bright X-ray emission region;

NGC is similar to others radio galaxies but its relative proximity and its core dominance in the radio band, to make more interesting to observe it also in the gamma-ray band. In reference to the radio/gamma-rays relation [15] we have estimated the flux of the source at 100 Mev as -13.2 $\pm$0.5ergcm^{-2}s^{-1}.

By considering the gamma-ray flux / radio flux ratio we have also estimated for NGC326 a gamma-ray flux of 0.2×10^{-12} ph cm^{-2} s^{-1} at 300 GeV.
It is necessary to note that the value of 0.26 for the core dominance in NGC 326 imply that the core radio power is lower than the value expected from the correlation; therefore the nuclear observed power is de-boosted [29].
Because the major part of the radio emission from NGC 326 is from the nucleus and not from the jets and from the lobes (core dominance), its future detection can imply that the gamma-ray emission is from this site.
When I started my PhD course I already knew that I would have studied the connection between the radio emission and the gamma-ray emission in the AGN, but I had not yet identified the predominant object of the investigation. I started by proposing the observation of this particular radio galaxy (which precisely emits in the bands optical, radio and X-ray) with the MAGIC gamma-ray telescope for a possible detection. Given the estimated sensitivity, I believe that the future CTA telescope will be able to detect it. The possible relationship between the radio emission and the gamma-ray emission in the AGN is probably localized (in the nucleus, in the jets or in the extended emissions); I believe that to be able to decipher it, we should also focus on particular "key objects".

References

[1] B. Acharya et al. Introducing the cta concept. *Astroparticle Physics*, (43):3, 2013.

[2] M. Ackemann et al. The second catalog of active galactic nuclei detected by the fermi large area telescope. *Astrophysical Journal*, (743):171, 2011.

[3] W. Atwood et al. The large area telescope on the fermi gamma-ray space telescope mission. *Astrophysical Journal*, (697):1071, 2009.

[4] W. Baade and R. Minkoswski. Identification of the radio sources in cassiopeia, cygnus a and puppis a. *Astrophysical Journal*, (119):206, 1954.

[5] Brown and M. Adams. High-energy gamma-ray properties of radio galaxy ngc1275. *Montly Notice of the Royal Astronomical Society*, (413):2785, 2011.

[6] Capetti et al. The host galaxy/agn connection in nearby early-type galaxies. *Astronomy and Astrophysics*, (440):73, 2005.

[7] T. Cheung. he agn population in radio and gamma-rays: Origins and present perspective. *Highlights of Astronomy*, (16):1, 2012.

[8] F. D'Ammando. To be or not to be a blazar. *Highlights of Astronomy*, (16):4, 2012.

[9] A. De Angelis, O. Mansutti, and M. Persic. Very-high-energy gamma astrophysics. *La Rivista del Nuovo Cimento*, (31):187, 2008.

[10] D. Donato et al. Hard x-ray properties of blazars. *Astronomy and Astrophysics*, (375):739, 2001.

[11] J. Fanaroff and J. Riley. The morphology of extragalactic radio sources of high and low luminosity. *Montly Notice of the Royal Astronomical Society*, (167):31, 1974.

[12] G. Fossati et al. A unifying view of the spectral energy distributions of blazars. *Montly Notice of the Royal Society*, (299):433, 1998.

[13] G. Ghirlanda et al. The radio/gamma-ray connection in fermi-blazars. *Montly Notice of the Royal Astronomical Society*, (411):901, 2011.

[14] G. Ghisellini and A. Celotti. Blazars, gamma ray bursts and galactic superluminal sources blazars, gamma ray bursts and galactic superluminal sources. *Blazars Astrophysics with BeppoSAX and other Observatories*, page 257, 2002.

[15] G. Ghisellini et al. Cosmology with gamma-ray bursts. *Astronomy and Astrophysics*, (432):401, 2005.

[16] M. Giroletti et al. The connection between radio and high energy emission in black hole powered systems in the ska era. *Proceedings of Advancing Astrophysics with the Square Kilometre Array*, (153), 2015.

[17] M. Giroletti and A. Polatidis. Sample of statistics of css and gps sources. *Astronomishe Nachiten*, (88):789, 2006.

[18] P. Grandi et al. Gamma-rays from radio galaxies. In *International Journal of Modern Physics: Conference Series*, 2011.

[19] F. Haardt and L. Maraschi. Theory of black hole accretion discs. *Astrophysical Journal*, (380):L51, 1991.

[20] D. Harris and H. Krawczynski. X-ray emission from extragalactic jets. *astro-ph*, page 1, 2006.

[21] M. Harwit. Cosmic discovery. the search, scope, and heritage of astronomy. *The MIT press*, page 1, 1981.

[22] Hodges-Kluck and A. Reynolds. The chandra view of nearby x-shaped radio galaxies. *Astrophysical Journal*, (710):1205, 2010.

[23] T. Hovatta. Assessing agn variability and cross-waveband correlations in the era of high-quality monitoring data in low and high energies. *Highlights of Astronomy*, (16):7, 2012.

[24] Y. Inoue et al. Agn population studies for cta. In *Proceedings of AGN Physics in the CTA Era, Toulouse, France*, 2011.

[25] M. Karouzos. Gamma-rays in flat-spectrum agn: revisiting the fast jet hypothesis. *Highlights of Astronomy*, (16):3, 2012.

[26] Y. Kovalev. Identification of the early fermi lat gamma-ray bright objects with extragalactic vlbi sources. *Astrophysical Journal*, (707):L56, 2009.

[27] M. Lister. Blazars at high resolution. *Highlights of Astronomy*, (16):5, 2012.

[28] X. Liu. Vlbi core flux density and position angle analysis of the mojave agn. *Highlights of Astronomy*, (16):8, 2012.

[29] Liuzzo et al. The bologna complete sample of nearby radio sources. *Astronomy and Astrophysics*, (505):509, 2009.

[30] S. Lombardi. Magic telescope observation of bllac objects. *Fermi Symposyum, Rome, May 9-12;*, 2011.

[31] W. Max-Moerbeck et al. Connecting radio variability to the characteristics of gamma-ray blazars. In *Proceedings of the IAU Symposium No. 313: "Extragalactic jets from every angle," F. Massaro, C. C. Cheung, E. Lopez, and A. Siemiginowska (Eds.), Cambridge University Press*, Galapagos, Ecuador, 15-19 September 2014.

[32] T. Muxlow and S. Garrington. Observations of large scale extragalactic jets. In C. U. Press, editor, *Beams and Jets in Astrophysics*, page 52, 1991.

[33] E. Nieppola et al. Blazar sequence. *Astronomy and Astrophysics*, (488):867, 2008.

[34] P. Nolan et al. The fermi large area telescope second source catalog. *The Astrophysical Journal Supplement*, (199):31, 2012.

[35] C. P. O'Dea. The compact steep-spectrum and gigahertz peaked- spectrum radio sources. *PASP*, (110):493, 1998.

[36] M. Orienti. Radio and gamma-ray connection in relativistic jets. In *Proceedings of the "12th European VLBI Network Symposium and Users Meeting - EVN 2014" (7-10 October 2014, Cagliari, Italy); published online in Proceedings of Science, PoS(EVN 2014)012*, 7-10 October 2014, Cagliari, Italy.

[37] M. Orienti et al. On the connection between radio and gamma rays. variability and polarization properties in relativistic jets. *Proceeding of the innermost regions of relativistic jets and their magnetic fields*, Granada, (Spain) 2013.

[38] M. Persic et al. Cta: the future of ground-based gamma-ray astrophysics. In *Proc. of 9th Workshop on Science with the New Generation of High-Energy Gamma-Ray Experiments (SciNeGHE 2012) held in Lecce, Italy, on June 20-22*, 2012.

[39] R. M. Prestage and J. A. Peacock. The cluster environments of powerful radio galaxies. *Montly Notice of the Royal Astronomical Society*, (230):131, 1988.

[40] M. Rees. Black hole models for active galactic nuclei. *Annual Review Astronomy and Astrophysics*, (22):471, 1984.

[41] J. L. Richards et al. Connecting radio variability to the characteristics of gamma-ray blazars. In *Proceeding of The innermost regions of relativistic jets and their magnetic fields*, Granada (Spain) 2013.

[42] E. E. Salpeter. Accretion of interstellar matter by massive objects. *Astrophysical Journal*, (140):796, 1964.

[43] C. K. Seyfert. Nuclear emission in spiral nebulae. *Astrophysical Journal*, (97):28, 1943.

[44] N. I. Shakura and R. A. Sunyaev. Black holes in binary systems. observational appearance. *Astronomy and astrophysics*, (24):337, 1973.

[45] Z. Shen. High precision position measurements of the cores in 3c 66a and 3c 66b. *Highlights of Astronomy*, (16):5, 2012.

[46] M. Sikora and G. Madejski. Learning about jets from observations of blazars. In P. C. Meudon, editor, *Active Galactic Nuclei: From Central Engine to Host Galaxy*, page 1, 2002.

[47] H. Sol. Active galactic nuclei under scrutiny of cta. *Astroparticle Physics*, (43):215, 2012.

[48] L. Stawarz. The agn population in radio and gamma rays: theoretical perspectives. *Highlights of Astronomy*, (16):2, 2012.

[49] F. Tavecchio. Variability of blazars: probing emission regions and acceleration processes. *Highlights of Astronomy*, (16):7, 2012.

[50] A. Tchekhovskoy. What sets the power of jets from accreting black holes? *Highlights of Astronomy*, (16):9, 2012.

[51] C. Urry and P. Padovani. Unified schemes for radio sources. *Publications of the Astronomical Society of the Pacific*, (107):803, 1995.

[52] E. Valtaoja. Gamma-ray emission along the radio jet: studies with planck, mets ahovi and fermi data. *Highlights of Astronomy*, (16):8, 2012.

[53] F. Xu-Liang et al. The connection between radio and gamma ray emission in fermi/lat blazars. *RAA*, (12):1475, 2012.

[54] Zaninetti. Physical mechanism that shape the morphologies of extragalactic jets. *Revista Mexicana de Astronomia y Astrofisica*, (43):59, 2007.

[55] A. Zech et al. Agn physics with the cherenkov telescope array. In *Fermi and Jansky Proceedings*, 2012.

[56] Y. Zeldovich. Observations in a universe homogeneous in the mean. *Sov. Astrron.*, (8):13, 1964.

Epilogo

"Lungi dall'essere una conoscenza incosciente, la cultura e' una trasformazione cosciente della natura." (Pape Gora Tall)